



THE UNIVERSITY *of* EDINBURGH

Edinburgh Research Explorer

A comprehensive review of hydrogen production and storage: A focus on the role of nanomaterials

Citation for published version:

Epelle, E, Desongu, K, Obande, W, Adeleke, A, Ikubanni, P, Okolie, J & Gunes, B 2022, 'A comprehensive review of hydrogen production and storage: A focus on the role of nanomaterials', *International journal of hydrogen energy*, vol. 47, no. 47, pp. 20398-20431. <https://doi.org/10.1016/j.ijhydene.2022.04.227>

Digital Object Identifier (DOI):

[10.1016/j.ijhydene.2022.04.227](https://doi.org/10.1016/j.ijhydene.2022.04.227)

Link:

[Link to publication record in Edinburgh Research Explorer](#)

Document Version:

Peer reviewed version

Published In:

International journal of hydrogen energy

General rights

Copyright for the publications made accessible via the Edinburgh Research Explorer is retained by the author(s) and / or other copyright owners and it is a condition of accessing these publications that users recognise and abide by the legal requirements associated with these rights.

Take down policy

The University of Edinburgh has made every reasonable effort to ensure that Edinburgh Research Explorer content complies with UK legislation. If you believe that the public display of this file breaches copyright please contact openaccess@ed.ac.uk providing details, and we will remove access to the work immediately and investigate your claim.



1 **A comprehensive review of hydrogen production and storage: A**
2 **focus on the role of nanomaterials**

3 Emmanuel I. Epelle¹, Kwaghtaver S. Desongu², Winifred Obande³, Adekunle A. Adeleke⁴, Peter
4 P. Ikubanni⁴, Jude A. Okolie⁵, Burcu Gunes⁶

5 ¹School of Computing, Engineering and Physical Sciences, University of the West of Scotland,
6 Paisley, United Kingdom.

7 ²Department of Chemical Engineering, Federal University of Technology, Minna Nigeria.

8 ³School of Engineering, Institute for Materials and Processes, The University of Edinburgh,
9 Robert Stevenson Road, Edinburgh, EH9 3FB, Scotland, United Kingdom.

10 ⁴Mechanical Engineering Department, Landmark University, Omu Aran, Nigeria

11 ⁵Department of Chemical and Biological Engineering, University of Saskatchewan, Saskatoon,
12 Saskatchewan, Canada.

13 ⁶School of Biotechnology and DCU Water Institute, Dublin City University, Glasnevin, Dublin,
14 Ireland

15
16
17
18
19 * **Corresponding author:**

20 Dr. Burcu Gunes

21 Assistant Professor in Bioprocess Engineering

22 School of Biotechnology

23 DCU Water Institute

24 Dublin City University

25 burcu.gunes@dcu.ie

26

27

1 List of Abbreviation

AC	Activated carbon
AER	Alkaline enhanced reforming
APR	Aqueous phase reforming
CCD	Central composite design
CMH	Complex metal hydrides
CMPs	Conjugated microporous polymers
CNT	Carbon nanotubes
CSHNSs	Core/shell heteronano structures
DFT	Density functional theory
DOE	US Department of Energy
ENME	Electrospun nanomaterials-based electrocatalysts
FT	Fischer-Tropsch
GDA	Generalized gradient approximation
GNP	Graphene nanoplatelets
HER	H ₂ evolution reaction
HTF	Heat transfer fluid
IRMOF	Isorecticular metal-organic frameworks
LCPs	Linear conjugated polymers
LDA	Local density approximation
MHHSS	Metal hydride based H ₂ storage system
MOF	Metal-organic framework
MWCNT	Multi-walled carbon nanotubes
OER	Oxygen evolution reaction
QCNs	Quantum Cu (II) nanodots
SMR	Steam reforming reaction
SWCNT	Single-walled carbon nanotube
TOF	Turnover frequency
WGSR	Water-gas-shift reaction

2

3

1 **Abstract**

2 Nanomaterials are beginning to play an essential role in addressing the challenges associated with
3 hydrogen production and storage. The outstanding physicochemical properties of nanomaterials
4 suggest their applications in almost all technological breakthroughs ranging from catalysis, metal-
5 organic framework, complex hydrides, etc. This study outlines the applications of nanomaterials
6 in hydrogen production (considering both thermochemical, biological, and water splitting
7 methods) and storage. Recent advances in renewable hydrogen production methods are elucidated
8 along with a comparison of different nanomaterials used to enhance renewable hydrogen
9 production. Additionally, nanomaterials for solid-state hydrogen storage are reviewed. The
10 characteristics of various nanomaterials for hydrogen storage are compared. Some nanomaterials
11 discussed include carbon nanotubes, activated carbon, metal-doped carbon-based nanomaterials,
12 metal-organic frameworks. Other materials such as complex hydrides and clathrates are outlined.
13 Finally, future research perspectives related to the application of nanomaterials for hydrogen
14 production and storage are discussed.

15 **Keywords:** Hydrogen; Nanomaterials; Electrolysis; Water splitting; Gasification, Activated
16 carbon.

17 **Word count: 11360**

1 **1. Introduction**

2 Recently there has been a tremendous increase in the number of researchers, scholars, countries,
3 and stakeholders considering hydrogen energy as a panacea for the increasing energy demand,
4 environmental pollution, and overdependency on fossil fuels. More specifically, the world is facing
5 greenhouse gas emissions, climate change, energy security, and water pollution challenges [1].
6 Therefore, developing alternative energy sources that are environmentally friendly and sustainable
7 over a long duration is imperative.

8 Hydrogen is preferred as an energy carrier and a promising alternative to carbon-based fuels due
9 to its renewability and pollution-free characteristics. It should be mentioned that hydrogen is
10 pollution-free when combusted because it does not have CO₂. However, its renewability and
11 "pollution-free" characteristics are based on the production routes. The combustion of H₂ of
12 hydrogen releases water vapour, and its calorific value (141.9 kJ/g) is three times more than that
13 of gasoline (47 kJ/g) and 2.6 times greater than natural gas (54 kJ/g) [2]. Compared with other
14 fuels such as ethanol and natural gas, hydrogen is lighter with a density of 0.08988 g/L at standard
15 temperature and pressure (STP) and a molar mass of 1.008 g/mole [3]. Moreover, the energy
16 density per volume of hydrogen (0.09 kg/m³) is relatively low at STP compared to other fuels.[3]
17 Due to the low volumetric energy density, storing hydrogen in vehicles requires a large tank at a
18 higher pressure than other gaseous fuels [4]. Therefore, it is imperative to develop advanced
19 storage technologies to increase energy density per volume. The lightweight properties of
20 hydrogen makes it a unique and versatile energy carrier with a broad spectrum of applications.
21 Okolie et al. [5] recently summarized different industrial applications of hydrogen. Although
22 hydrogen is a promising fuel, its production and storage are associated with several technical and
23 scientific challenges that impede its worldwide implementation [6].

24 Steam reforming of natural gas (SMR) is a widespread hydrogen production method. However,
25 Acar and Dincer's [6] studies reveal that fossil-based hydrogen production is one of the most
26 environmentally harmful processes. As such, there is an urgent need to develop large-scale, cost-
27 effective, renewable, and ecologically benign hydrogen production processes.

28 Another challenge, as noted earlier, is associated with the lack of practical, easy, safe and cheap
29 storage methodologies [7]. Additionally, the onboard storage of hydrogen in vehicles is another
30 bottleneck because of the stringent requirements in its storage. Currently, hydrogen is often stored
31 in the gaseous or liquid form in pressurized or cryogenic tanks [8]. However, these technologies

1 do not meet the requirements of large-scale storage. Therefore, there is a need to develop cost-
2 effective, reliable, and safe storage systems to foster the development of a hydrogen economy.
3 Engineered nanomaterials have a size ranging from 1-100 nm and are produced and designed
4 specifically to simulate their properties for specific applications. Nanomaterials are beginning to
5 play a significant role in the development of new fields in addition to their tremendous impact on
6 improving hydrogen production and storage [9].
7 Several studies have evaluated different areas where nanomaterials could improve hydrogen
8 production and storage. Reddy et al. [9] reported recent research progress in the use of plasmonic
9 photocatalyst nanoparticles for hydrogen production. Mao et al. [10] reviewed the application of
10 different nanostructured materials for renewable hydrogen production, storage, and utilization.
11 However, the review is solely focused on solar hydrogen production and does not consider
12 renewable hydrogen from biomass conversion processes [10]. Recently, Abdalla et al. [11] outlined
13 hydrogen production and storage challenges and prospects. However, recent advances on nano-
14 based materials for hydrogen storage and production were lacking. This has partly motivated the
15 work herein. To the best of the authors' knowledge, there is no comprehensive review that
16 summarizes the advancement in the use of nanomaterials for hydrogen production and storage.
17 Therefore, this study outlines the applications of nanomaterials in hydrogen production
18 (considering both biological and water splitting methods) and storage. Other materials such as
19 complex hydrides and clathrates used for hydrogen storage are also outlined in this study.
20 This review is organized as follows. The first section starts with the introduction, after which the
21 methodology is briefly outlined. Different hydrogen production methods are comprehensively
22 discussed in Section 3. The next section outlines various studies related to the application of
23 nanomaterials for renewable hydrogen production with a focus on biological and thermochemical
24 conversion processes. In Section 5, different hydrogen storage methods are discussed and
25 compared. Section 6 reviews previous research on the application of various nanomaterials to
26 facilitate hydrogen storage. The study ends with a conclusion and future perspectives.

27 **2. Methodology**

28 Google Scholar, Scopus, Web of Science, and PubMed were used as search engines for the initial
29 search. The following keywords and/or phrases were used: complex metal hydrides, hydrogen
30 storage nanomaterials, limitations of hydrogen storage, nanomaterials for renewable hydrogen
31 storage, hydrogen storage nanoconfinement nanoelectrocatalysts, nanophotocatalysts, carbon

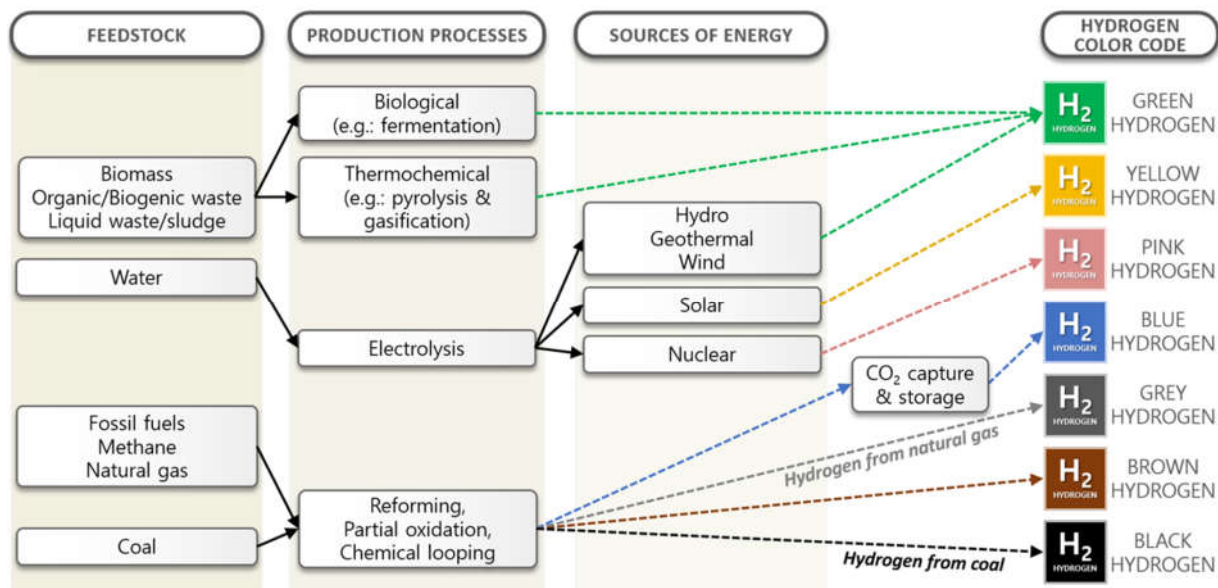
1 nanotubes, catalytic nanomaterials, carbon-based nanocomposites, carbon cryogel
2 nanocomposites, fullerene-based nanocomposites, and metal organic framework. The search was
3 narrowed down to two categories. Category 1 is for articles published within the last eight years
4 to ensure that the information presented is recent and relevant. The second category is for articles
5 published in the 30 years to provide the readers with the research progress and pioneering findings
6 in nanomaterials for hydrogen production and storage.

7 The articles were screened into two subcategories. In screening Category 1, studies related to the
8 application of nanomaterials to renewable hydrogen production were considered. Category 2
9 focuses specifically on the applications of nanomaterials for hydrogen storage. Literature
10 screening was performed by an initial reading of the articles' title, abstract, and conclusions to
11 obtain the overall scope and objectives. Based on this, articles that fit the objectives of this study
12 were selected. About 120 papers were chosen to fit the criteria.

13 **3. Hydrogen production routes**

14 Pure hydrogen hardly exists alone due to its high reactivity; instead, it is attached to carbon and
15 oxygen in various compounds such as hydrocarbons, water, etc. A significant quantity of energy
16 is needed to separate hydrogen from such compounds. Based on the separation methods,
17 conversion processes, and the feedstock used for hydrogen production, colour codes such as green,
18 grey, black, and blue are used, as shown in Fig.1. The hydrogen produced from natural gas via
19 steam reforming without carbon capture and storage (CCS) is called grey hydrogen. Moreover, if
20 bituminous or lignite coal is used as feedstock, the hydrogen is called black or brown hydrogen
21 [12]. Steam reforming of natural gas coupled with CCS produces blue hydrogen. This type of
22 hydrogen is carbon neutral if all the CO₂ is captured and stored underground. However, the process
23 is termed “low carbon” if CO₂ is not captured completely. Hydrogen produced from electrolytic
24 splitting using clean energy sources such as wind is green hydrogen [13]. Thermochemical and
25 biological conversion processes also produce green hydrogen. Integrating biomass conversion
26 processes with CCS produces even more greener hydrogen with negative CO₂ emissions.

27

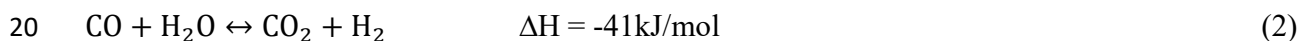
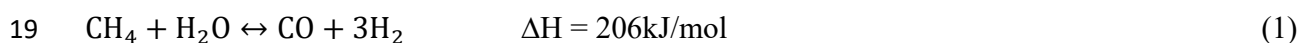


1
2 **Figure 1:** Hydrogen production routes and the associated colour codes (Note: the colour codes
3 presented here are solely based on the present authors' perspectives and experiences, moreover
4 naming convention and colour codes often differs across countries and over time.

5 **3.1 Reforming reactions (steam, aqueous, alkaline enhanced, and autothermal** 6 **reforming)**

7 Steam reforming reaction (SMR) is the dominant process for large-scale hydrogen production,
8 accounting for more than 59% of the global production from fossil fuels (natural gas, heavy
9 oils/naphtha, and coal). The other common methods for hydrogen production from fossil fuels are
10 alkaline enhanced reforming, aqueous reforming, and autothermal reforming [14].

11 SMR refers to the conversion of the hydrocarbons, usually methane and steam, into hydrogen and
12 carbon dioxide at high temperatures (~800 °C) in the presence of a catalyst and under pressure
13 (~3.5 MPa) (Equation 1). The CO present in the syngas also reacts with water to produce hydrogen
14 and carbon dioxide through the water-gas-shift reaction (WGSR) (Equation 2) [15]. The produced
15 gas mixture is then sent to sequential purification steps to achieve 100% hydrogen purity. To
16 prevent catalyst poisoning, an additional desulphurization stage is required for high sulphur
17 feedstocks before syngas generation [14]. Several metal catalysts such as Co, Ni, Rh, and Pt have
18 been used to elevate hydrogen yield from steam reforming reactions [16,17].



1 Aqueous phase reforming (APR) of different types of oxygenated hydrocarbons such as glycerol,
2 methanol, ethanol, or propanol is another route for hydrogen production. The process occurs in the
3 presence of a metal catalyst at moderate temperature (225–265°C) and pressures (27–54 bar) [18].
4 Under these conditions, steam formation is inhibited, and the reaction would proceed in the
5 aqueous phase. The APR produces high hydrogen yield and low CO yield due to its ability to
6 thermodynamically promote WGSR [19]. APR process with biomass-based feedstock has been
7 reported by several researchers [16,19,20]. A recent experimental study proposed a novel pathway
8 that utilized the aqueous liquid from Fischer-Tropsch (FT) synthesis to produce biohydrogen
9 through APR [21].

10 Alkaline enhanced reforming (AER) is another approach used to convert water-containing
11 organics into hydrogen at low temperatures (<220 °C) and pressures in an alkaline medium
12 (usually NaOH). The addition of an alkaline ensures that the reaction medium maintains a basic
13 pH to create an environment that promotes conventional SMR [18]. The carbon produced from
14 APR precipitates as solid Na₂CO₃ rather than gaseous pollutants (CO and CO₂) in SMR. Therefore,
15 APR produces fewer greenhouse gases and is more environmentally friendly.

16 Partial oxidation, autothermal reforming, combined steam methane reforming with partial
17 oxidation are also promising hydrogen production methods from hydrocarbons. During
18 autothermal reforming, the hydrocarbon feed is partially oxidized in the presence of oxygen and
19 steam to produce hydrogen-rich syngas [22].

20 **3.2 Thermochemical Processes**

21 Thermochemical processes for hydrogen production such as pyrolysis and gasification use heat
22 and chemical reactions to decompose organic materials into hydrogen [23]. During pyrolysis,
23 biomass is converted to bio-oil, char, tar, a mixture of H₂, CO, CO₂, and hydrocarbons in an
24 oxygen-depleted environment at around 400 °C and 0.1-0.5 MPa [24]. Increased hydrogen
25 production can be achieved by reforming the pyrolysis by-products such as aqueous liquid (bio-
26 oil) or further conversion of the CO in the gaseous product to produce more hydrogen via WGSR.
27 The pyrolysis gas mixture is purified, typically by a pressure swing adsorption or a CO₂ removal
28 process [14]. Reaction temperature, residence time, and most importantly, the type of biomass and
29 catalyst used in the process are the key factors affecting hydrogen yield during pyrolysis [25,26].
30 Based on these factors, pyrolysis can be classified as slow, fast, or flash, as detailed and compared
31 in Table 1.

1 **Table 1:** Comparisons between different types of pyrolysis and hydrothermal liquefaction Nanda et al.
 2 [2], Okolie et al. [5]

Biomass conversion processes	Main products	Residence time (s)	Reaction temperature (°C)	Biomass particle size (mm)	Heating rate (°C/s)
Fast pyrolysis	Biochar < Gases < Bio-oil	0.5 – 10	400 – 800	< 1	10 – 200
Slow pyrolysis	Gases < Bio-oil < Biochar	600 – 6000	300 – 700	5 – 50	0.1 – 1
Flash pyrolysis	Biochar < Gases < Bio-oil	< 0.5	800 – 1000	< 0.2	1000

3

4 Gasification is a thermochemical process that converts organic matter into hydrogen-rich syngas
 5 at high temperatures and can be either conventional or hydrothermal (also known as supercritical
 6 water gasification). Although both conventional and thermochemical gasification processes are
 7 comparable in terms of the desired product, they differ based on the composition of the gaseous
 8 products and the operating conditions. In conventional gasification, biomass is converted to syngas
 9 (mixture of H₂, CO, CO, CH₄, and other hydrocarbons), tar, and char in the presence of a gasifying
 10 agent like oxygen and/or steam. The process occurs at an operating temperature and pressure range
 11 of 500-1400 °C and 0-4 MPa, respectively [27]. The process yield is mainly dependent on the type
 12 of biomass, type of catalyst, particle size, steam-to-biomass ratio, and reaction temperature
 13 [28,29].

14 Hydrothermal gasification is the thermochemical conversion of organic materials into hydrogen-
 15 rich syngas under supercritical conditions (temperature > 374 °C, pressure > 22.1 MPa) [30]. Water
 16 displays unique physicochemical properties such as gas-like viscosity and liquid-like density at
 17 supercritical conditions, leading to improved dissolution and mass transfer [31,32]. Despite being
 18 more advantageous in terms of improved hydrogen yield and the ability to handle wet feedstock
 19 without drying, hydrothermal gasification has several challenges limiting large-scale production.
 20 The high temperatures and pressures needed to attain supercritical conditions lead to an elevation
 21 in the operating cost compared with other biomass conversion technologies [23] and potential
 22 noise, explosion, injury, and odour risks [33,34].

1 **3.3 Biological processes**

2 Biological processes use microorganisms to decompose organic matter into hydrogen. Examples
3 of such processes include biophotolysis and dark/photo fermentation. Biological hydrogen
4 production processes have attracted global research interest owing to their applicability at ambient
5 operating temperatures and pressures and waste recycling ability [35].

6 In direct biophotolysis, water undergoes prior splitting into hydrogen and oxygen ions by the
7 photosynthetic activity of green algae. The hydrogen ions are then converted into H₂ (hydrogen
8 gas) by the hydrogenase enzyme [36] under strictly anaerobic conditions (O₂ content <0.1%) due
9 to the extreme enzyme sensitivity [37]. The major drawbacks of the biophotolysis process are
10 complex bioreactor design with large surface areas for light capturing and low hydrogen
11 conversion yields [36,38].

12 On the other hand, fermentative processes achieve simultaneous organic waste treatment and
13 hydrogen production via microbial biomass transformation with or without oxygen [14]. In the
14 metabolic process of dark fermentation, sequential carbon chain reactions are carried out by the
15 obligate and facultative anaerobic bacteria to convert organic substrates into hydrogen, ethanol,
16 and volatile fatty acids in the absence of light [36]. An initial pre-treatment step might be required
17 to increase glucose digestibility when recalcitrant lignocellulosic biomass is used as a substrate
18 [14]. For successful operations, pH should be maintained in a range of 5-6, and the produced
19 hydrogen should constantly be removed from the system to stimulate the hydrogenase enzyme
20 [37,38].

21 Photo-fermentation relies on the nitrogenase enzyme in photosynthetic bacteria to convert organic
22 acids into H₂ and CO₂ [39]. In the case of using industrial wastewater as the substrate, an additional
23 pre-treatment step is required for heavy metal and colour removal to attain sufficient light
24 penetration [36]. Although photo-fermentation achieves higher theoretical H₂ production yields,
25 the limited availability of organic acids, low efficiency in solar energy conversion, and
26 complicated bioreactor demand with large surface areas are major limitations of this technology
27 compared with dark fermentation [37,38]. Nonetheless, higher H₂ production yields with minimum
28 solar energy dependency can be achieved by an integrated sequential dark/photo fermentation
29 system with anaerobic and photogenetic bacteria.

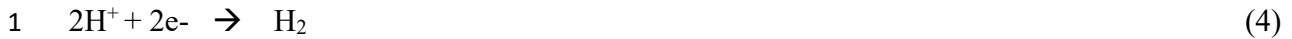
1 **3.4 Hydrogen production through water splitting**

2 Water splitting involves water decomposition into H₂ and O₂ through a reaction involving charge
3 carriers. This promising H₂ generation process has improved over time, and there are currently
4 four distinct methods explored for this purpose; these include thermochemical (thermolysis),
5 electrochemical (electrolysis), photochemical (photolysis), and photoelectrochemical methods
6 [40]. These methods are still subjected to ongoing research and are at different levels of
7 development. The thermolysis process is very similar to electrolysis except for the use of thermal
8 energy for water splitting instead of electricity.

9 Thermochemical water splitting involves the decomposition of water into O₂ and H₂ through
10 repetitive series of chemical reactions, usually at temperatures between 500–2000°C [41]. In
11 theory, heat is the only form of energy required for this reaction to occur, as every other resource
12 is recycled and reused. As a result of the high heat energy requirement, the process is costly.
13 Therefore, it has limited its application in the large-scale production of H₂, despite offering more
14 than 77% efficiency [40,41]. During thermochemical water splitting, the water should be heated
15 above 2500°C to achieve hydrogen separation [14]. Besides, several thermolysis cycles (Cu-Cl
16 and Mg-Cl) are preferred to help lower the reaction temperature. In these cycles, sequential
17 chemical reactions are carried out at different temperatures where the heat is converted into a
18 chemical energy carrier in the form of H₂ [42,43].

19 Electrochemical water splitting involves splitting water into H₂ and O₂ by the passage of electrical
20 energy in electrochemical cells. A typical electrolysis unit consists of an anode (negatively
21 charged) and cathode (positively charged) probes submerged in an electrolyte. Following the
22 passage of electric current, H₂ is produced in the cathode while O₂ accumulates around the anode
23 [44]. The redox reaction, where two half-reactions occur simultaneously, is one of the most
24 promising methods of renewable H₂ production. An oxidation half-reaction, commonly called
25 oxygen evolution reaction (OER), occurs at the anode of the electrochemical cell. In contrast, a
26 reduction half-reaction, commonly called H₂ evolution reaction (HER), occurs at the cathode of
27 the electrochemical cell. The OER and HER are represented by Equations 3 and 4, respectively.





2 Alkaline, proton exchange membrane, and solid oxide electrolysis cells are currently the most
3 developed technologies for pure hydrogen production from water splitting. However, the
4 electrochemical reactions are extremely endothermic, leading to high electricity consumption,
5 rendering these technologies economically unfeasible [14].

6 The photolysis process is very similar to electrolysis; however, the energy requirement of the water
7 splitting is provided by the absorbed sunlight by the semiconducting materials. An electron-hole
8 pair is produced and separated due to the electric field between the electrolyte and semiconductor.
9 The holes stay at the anode and decompose water into hydrogen ions (H^+) and oxygen. The H^+
10 travels to the cathode through the electrolyte, while the electrons travel through an external circuit
11 to react with the H^+ at the cathode to produce H_2 [45].

12 Water splitting can also be caused by sunlight and electricity, in the presence of photocatalysts
13 [46] absorbing sunlight to generate electrons and holes. The charges are separated and migrate to
14 the catalyst's surface. After that, a surface reaction with the H_2O molecules occurs, facilitating
15 water splitting into H_2 and O_2 (redox). In most cases, photocatalysis requires a sacrificial (electron)
16 donor that removes the photogenerated holes from the catalyst [40]. The sacrificial donors, which
17 are primarily carbon-based molecules, get oxidized in the process to form CO_2 . This has
18 environmental implications and must be addressed to make the process more attractive. There is,
19 therefore, a recommendation that the term "water splitting" should not be used when a sacrificial
20 donor is involved [40]. In addition, there are also concerns about the low conversion efficiency,
21 high cost of conversion, and unstable catalysts associated with photocatalytic water splitting [46].
22 These concerns indicate that there is substantial progress required before photocatalytic water
23 splitting becomes a credible and sustainable alternative for hydrogen production.

24 Photoelectrochemical hydrogen production involves splitting water with sunlight and specialized
25 semiconductors called photoelectrochemical materials [40]. The semiconductor materials are
26 similar to those used in photovoltaic solar electricity generation. However, they are immersed in a
27 water-based electrolyte in which sunlight facilitates the water-splitting process. The process is
28 promising because it can produce cost-effective hydrogen with improved conversion efficiency.
29 However, the current limitations are the semiconductor materials' durability, cost, and lifetime and

- 1 low sunlight absorption [47]. Table 2 outlines the advantages and limitations of different hydrogen
- 2 production methods discussed in this section.

Table 2: Major advantages and disadvantages of different hydrogen production technologies

	Advantages	Disadvantages
<u>Fossil Fuel Treatment</u> Steam reforming Partial oxidation Autothermal steam reforming	<ul style="list-style-type: none"> • Most established industrial process. • Higher production yields. • Economically more feasible. • High purity hydrogen is produced. 	<ul style="list-style-type: none"> • Causes massive GHG emissions and increased carbon footprint. • Limited feedstock availability due to the depletion of fossil fuels. • High operation temperature requirement • Lack of adequate carbon capture storage technologies (CCS). • Catalyst poisoning due to sulphur-containing feedstock.
<u>Thermochemical Processes</u> Gasification Pyrolysis	<ul style="list-style-type: none"> • Higher production yields than biological processes. • CO₂ neutral • Sustainable feedstock supply. • Short hydraulic retention times. • Negative CO₂ emission when CCS is used. 	<ul style="list-style-type: none"> • High operation temperature requirement. • Increased tar formation. • Varying H₂ content based on biomass seasonality and impurities.
<u>Biological Processes</u> Biophotolysis Dark/photo fermentation	<ul style="list-style-type: none"> • Sustainable feedstock availability • Negative CO₂ emission when CCS is used. • More environmentally friendly than fossil fuel production routes and thermochemical processes • Less energy-intensive due to mild operating conditions • Provides H₂ production and waste treatment simultaneously (fermentation). 	<ul style="list-style-type: none"> • Low production yields and rates • Long hydraulic retention times requirement • Difficulty in maintaining process stability • High O₂ sensitivity • Large surface area requirement for collecting adequate light (biophotolysis) • No waste recycling (biophotolysis)
<u>Water splitting</u> Electrolysis Thermolysis Photolysis Photoelectrochemical	<ul style="list-style-type: none"> • Sustainable feedstock supply • O₂ is the sole by-product • CO₂ neutral 	<ul style="list-style-type: none"> • High investment and operational costs • Low conversion efficiency • Corrosion problems • Sunlight demand (photolysis)

4. Nanomaterials for renewable hydrogen production

4.1 Nanoelectrocatalysts

The application of nanomaterials has gained popularity in electrochemical, photochemical, and photoelectrochemical water splitting. Electrocatalysts have a crucial role in facilitating water splitting to unlock its full potential of producing pure hydrogen that can meet the world's fast-growing energy demand. This is because the two half-reactions of water splitting – HER, and especially OER, are kinetically limited, requiring electrocatalysts to speed them up as well as to make them less energy-consuming [40].

Nanomaterials are taking centre stage in recent electrocatalytic and photocatalytic research because they exhibit desirable and tenable mechanical and electrical properties, offering large surface areas that significantly lower energy barriers and promote electron transfer at the electrodes. For instance, electrospun nanomaterials-based electrocatalysts (ENME) can undergo electronic modulation and interface engineering to enhance their catalytic performance [48]. Electronic modulation refers to catalyst doping with heteroatoms, while interface engineering is the construction of hybrids with unique interfaces that can contribute to more active sites on the catalysts.

Pt-group-metal-based electrocatalysts (Pt, Pd, Ru, Ir, and Rh) have proven to be excellent nanoelectrocatalysts for water splitting hydrogen production [49]. However, they are scarce, expensive, vulnerable to electrocatalysis poisoning, and tend to agglomerate [50], preventing their commercial application. Therefore, researchers are focusing on improving the catalytic efficiencies of non-noble metal-based electrocatalysts for water splitting-based hydrogen production since they are cheaper and more earthly abundant [50,51]. Some popular non-noble metal elements under study are Ni, Co, P, Fe, Cu, C, N, Se, W, Mo, and S. Table 3 shows some notable, recent findings of nanoelectrocatalysts for water splitting hydrogen production.

1 **Table 3:** Summary of some recent research contributions on nanoelectrocatalytic generation of H₂.

Reference	Approach	Overpotential	Current density	Tafel slope	Comments
Kumar et al. [51]	Experimental assessment using Teflon-lined autoclave and centrifuge	1.4 – 2.0 V	1 – 10 mA cm ⁻²	134 and 152 mVdec ⁻¹ (HER)	A multi-step solvothermal process was used to synthesize multi-shelled NiO/Ni/Graphene and Co ₃ O ₄ /Co/Graphene nano-spheres from MOFs, producing a highly efficient and stable catalyst for both HER and OER in acid media. The Co-based catalyst proved more efficient.
Narwade et al. [49]	Experimental assessment via morphological characterization (TGA, TEM, FESEM, EDAX, XRD)	582 mV for HER in an acidic medium	10 mA cm ⁻²	63 mVdec ⁻¹ for HER in an acid medium; 41 mVdec ⁻¹ for OER in basic media	A bifunctional, noble metal-free electrocatalyst was synthesized by a chemical process using Ni/NiO on reduced graphene oxide (Ni/NiO @ rGO).
Wang et al. [52]	An experimental study using HRTEM	325-540 mV for OER and 337-404 mV for HER in an alkaline media.	10 mA cm ⁻²	97-157 mVdec ⁻¹ (HER); 65-162 mVdec ⁻¹ (OER)	A promising, high-active and stable bifunctional electrocatalyst (CeNiFeO _x) was proposed using a facile one-pot combustion approach. A new height of 20% solubility of Ni/Fe in the ceria lattices was achieved for the first time. Ce _{0.8} Ni _{0.15} Fe _{0.05} O _x showed more excellent bifunctional catalytic performance.
Wan et al. [53]	Experimental assessment via electrostatic spinning and characterization	133 mV for HER in an acidic medium	10 mA cm ⁻²	—	CoSe ₂ nanostructured particles were synthesized on 3D nano-netlike carbon fibres (CoSe ₂ -CFN) by a spinning technique. The CoSe ₂ -CFN is characterized by high CoSe ₂ particle dispersion, high electrical conductivity, and catalytic activity.
Han et al. [54]	An experimental study via FE-SEM, EDS, TEM and XRD)	290 for OER and 77 mV for HER, in alkaline media.	10 mA cm ⁻²	56 mVdec ⁻¹	Cobalt phosphide incorporated with Vanadium (CoVP) self-supported catalyst on carbon cloth (CoVP@CC) was proposed in the study as a highly efficient, bifunctional electrocatalyst for OER and HER in alkaline medium.
Jadhav et al. [55]	Experimental study using electrosynthesis.	240 and 401 mV for OER and HER.	100 mA cm ⁻²	189 mVdec ⁻¹ (OER); 103	This study fabricated an organic-inorganic nanohybrid, namely BSeF/Ni(OH) ₂ , using one-step reductive electrosynthesis. The synthesized BSeF/Ni(OH) ₂ was

				mVdec ⁻¹ (HER)	demonstrated to be a bifunctional electrocatalyst with an excellent performance:
Yan et al. [56]	Experimental and theoretical study using VASP (Vienna <i>ab initio</i> Simulation Package)	67mV (HER) in acidic media and 89 mV (HER) in basic media.	10 and 100 mA cm ⁻²	57 mVdec ⁻¹ and 82 mVdec ⁻¹ in acidic and basic media.	A self-supported, hierarchical, and edge-rich electrocatalyst from nickel phosphide nanosheets arrays on nickel foam (Ni ₂ P NSs) showed highly efficient catalytic ability for HER in both acidic and basic media.
Dai et al. [57]	Experimental / Density Functional Theory (DFT)	171 and 243 mV for HER and OER, respectively	10 mA cm ⁻²	28.1 mVdec ⁻¹	A new bifunctional electrocatalyst for water splitting was found in CoNi ₂ S ₄ /Ni ₃ S ₂ on nickel foam (CoNi ₂ S ₄ /Ni ₃ S ₂ @NF) in alkaline media. The obtained electropotentials supersede those of metallic NF and Ni ₃ S ₂ separately. DFT calculations showed that the strong coupling between CoNi ₂ S ₄ and Ni ₃ S ₂ improves the electrochemical performance.
Kumar and Bhattacharyya. [58]	Experimental assessment applying thermal treatment in air.	271 and 197 mV for OER and HER in alkaline medium	10 mA cm ⁻²	48 mVdec ⁻¹ (OER); 130 mVdec ⁻¹ (HER)	A bifunctional electrocatalyst for efficient water splitting was manufactured from porous NiFe-oxide nanocubes (NiFe-NC). It also shows corrosion-resistant properties for water splitting, in addition to its long-term stability.
Zeng et al. [59]	Experimental in combination with DFT	80 and 210 mV for HER and OER, respectively	10 mA cm ⁻²	65 mVdec ⁻¹ (HER); 62 mVdec ⁻¹ (OER);	A nanoelectrocatalyst was produced through a formation of a 3D-heterogeneous-nickel phosphide and its sulphide (Ni ₂ P and Ni ₃ S ₂) on nickel foam (Ni ₂ P/Ni ₃ S ₂ @NF), which enhances its catalytic performance for water splitting in alkaline media.
Mugheri et al. [60]	Experimental study on a solarton potentiostat	0.31 V	10 mA cm ⁻²	42 mVdec ⁻¹	Pristine SnCo and Cu-doped SnCo nanoelectrocatalysts were synthesized and studied. Cu-doped with 46% Cu showed an excellent HER catalytic performance comparable to the precious Pt/C.
Wang et al. [61]	Experimental in a Teflon-lined stainless-steel autoclave)	117 mV for HER	10 mA cm ⁻²	66 mV dec ⁻¹	MoSe ₂ @Ni _{8.85} Se electrocatalyst was shown to have excellent conductivity and abundant exposed sites that greatly improved HER in an alkaline medium.

1 Some key parameters that can be used to measure and compare nanoelectrocatalysts performances
2 include, but are not limited to: overpotential values (mV), Tafel slopes (mVdec^{-1}), turnover
3 frequency (TOF), binding energy for reaction intermediates, adsorption free energy (eV), Faradaic
4 efficiencies (%), electrochemical surface area (cm^2), stability time with unchanging overpotential,
5 mass activity (mAcm^{-1}), specific activity (mAcm^{-1}), charge transfer resistance (ohm), disruption
6 of electronic, electron density at the Fermi level. It is also important that suitable
7 nanoelectrocatalysts are bifunctional, environmentally friendly, and inexpensive to minimize
8 hydrogen production costs by water splitting while maintaining a safe environment. Currently, no
9 single catalyst possesses all the characteristics mentioned above [48,50,62].

10 While electrocatalysts and photocatalysts are both applied to catalyze water-splitting reactions for
11 hydrogen production, they have notable differences in properties [63]. Electrocatalysts utilize
12 externally induced electrical energy, and photocatalysts use solar energy. Qian et al. [63]
13 highlighted the superior performance of electrocatalysts compared to photocatalysts and other
14 differences between them. Nonetheless, this review expounds on the performance of a wide range
15 of electrocatalysts for H_2 production based on recent research contributions, as shown in Table 3.
16 Subsequently, it presents a detailed review of photocatalysts for H_2 production in Section 4.2.

17 **4.2 Nanophotocatalysts**

18 Generally, photocatalytic H_2 generation can be attained via photo splitting of water or photo
19 reforming of organic species [64,65]. These processes usually require catalysts capable of
20 absorbing radiation in the visible range and exciting electrons to the energy level needed for H_2
21 production [64]. Some nanomaterials, which are currently used for the photocatalytic production
22 of H_2 include SiC, TiO_2 , CdS, and CuInSe_2 , which can be generally categorized into metal-oxide
23 (such as TiO_2 and WO_2) and non-metal oxide (such as $\text{g-C}_3\text{N}_4$, B_4C , CuInSe_2 , and CdS)
24 photocatalysts [66]. The current attainable H_2 productions efficiencies (solar-to-fuel) using these
25 photocatalysts are low and far from meeting the required operational requirements for industrial
26 applications [64].

27 Research advancements in the field of photocatalytic water splitting have led to the development
28 of more than 100 new catalysts, including carbides, sulphides, and oxides [67]. Despite these
29 advancements, several challenges affecting their industrial applicability still exist. Some of these

1 include the selective activeness of photocatalysts to ultraviolet light (low visible-light quantum
 2 efficiency), rapid recombination of photogenerated charges, poor durability and physicochemical
 3 stability, high toxicity, and difficulty in preparing the catalyst on a large scale [68–70]. The factors
 4 affecting the performance of nanophotocatalysts for water splitting are outlined in Table 4.

5 **Table 4:** Factors affecting nanophotocatalyst performance and selection Bhatt and Lee. [66],
 6 Ganguly et al. [70].

Factors based on photocatalyst conversion efficiency	Factors based on practical application & operating conditions of the photocatalytic process
Extent of light absorption (specific photoactivity $> 10^4 \mu\text{moles H}_2/\text{h.g}$ –	Resistance and stability under visible light (photohydrostability without undergoing photocorrosion in aqueous solution).
Bandgap and exciton generation/charge mobility.	Nature of co-catalyst and preparation method.
Ability to promote H-O bond cleavage via a reduction of the reaction energy barrier (500 kJ/mol).	pH and operating temperature.
The extent of separation and recombination of photogenerated holes and electrons (charge carriers).	Size and shape tunability of photocatalyst particles, including morphology/structure and crystallinity.
Charge collection rate at electrodes.	The concentration of sacrificial agent (photoreforming).
Specific area (1D or 2D nanostructure)	Cost-effectiveness
The removal of nanoarchitectures by photons so that they reach the reactive site	Toxicity level
Suitability of sacrificial electron donor	Suitability for large scale preparation

7
 8 Poor light absorption and insufficient charge separation are the main reported factors; these are, in
 9 turn, a consequence of large bandgaps of the photocatalysts [71,72]. These large band gaps (mainly
 10 associated with metal oxides) often lie outside the visible light region in the electromagnetic
 11 spectrum [66]. Hence, they are incapable of utilizing the solar spectrum, regardless of their highly
 12 active catalytic properties (photocatalysts, which are active under visible light, are more efficient
 13 and effective because visible light constitutes a significant portion of electromagnetic radiations)

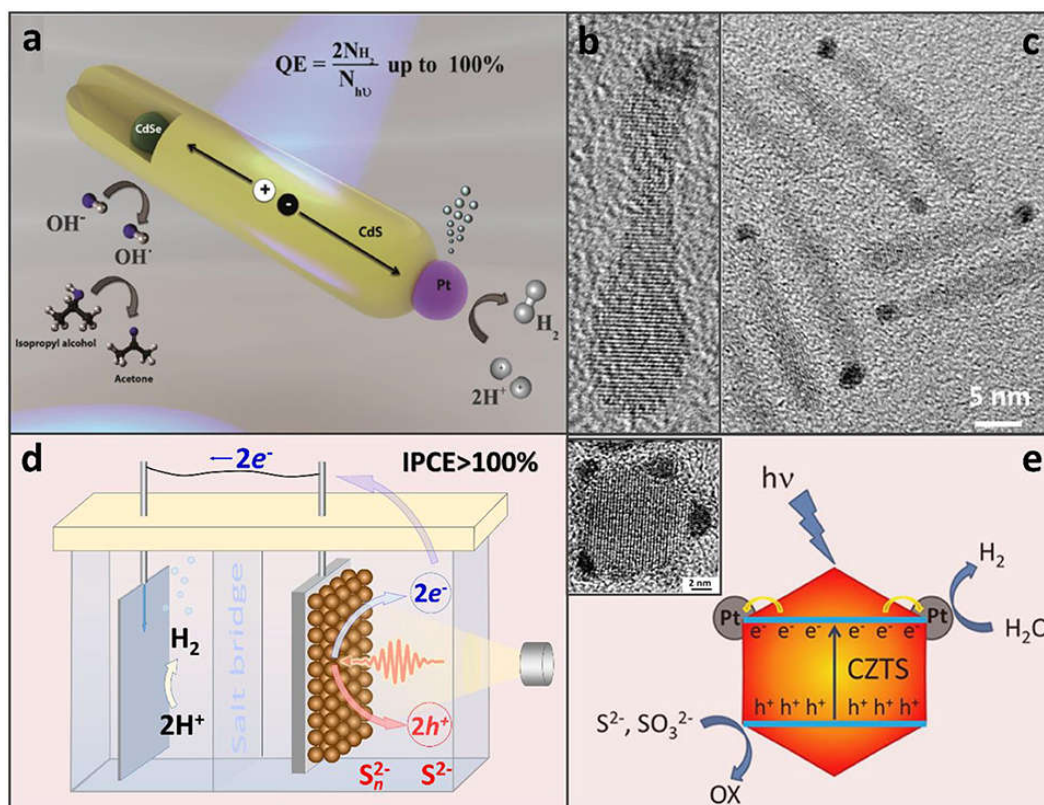
1 [71]. For instance, TiO_2 (with a bandgap of 3.2 eV) is limited to a solar-to- H_2 conversion efficiency
2 of 1%, whereas Fe_2O_3 (with a 2.2 eV bandgap) has a theoretical efficiency of 15% [66,73].

3 Some of the popular photocatalysts include a group of materials known as graphitic carbon
4 nitrides, conjugated microporous polymers (CMPs), linear conjugated polymers (LCPs), and
5 covalent organic frameworks [69,71,74]. Among these photocatalysts, graphitic nitrides (g- C_3N_4),
6 which belong to the class of organic semiconductors) have been widely studied. They have
7 emerged as viable candidates for solar-driven H_2 production via water splitting [75]. This may be
8 attributed to their optoelectronic properties and reduced environmental footprints compared to
9 inorganic and metal-complex materials. However, their inherent large molecular structures often
10 yield bulky particles in water, which are higher than the penetration length scale of light [69]. The
11 inevitable effect of this bulkiness is significantly optical losses, which ultimately reduce the
12 catalytic performance. Thus, the particle size of the photocatalyst is a predominant factor affecting
13 the catalyst's performance.

14 The size reduction of the particles to a few tens of nanometres can enhance their photocatalytic
15 performance [76]. Enhancing photocatalytic performance can be done using specialized methods
16 like nano-structure engineering to achieve thin layer nanosheets from bulk g- C_3N_4 [68,71]. Some
17 of the methods include physical exfoliation (liquid and chemical), emulsion polymerization,
18 sonification, template synthesis, and nanoprecipitation of polymer dots. Further details of these
19 methods are provided by Mahzoon et al. [68]. Moreover, the anisotropic 1D nanostructures have
20 been adopted in several studies due to the different behaviours of charge carriers obtained in
21 different directions. One dimensional hierarchical structure comprising of Ni_3S_2 nanosheets grown
22 on a carbon nanotube backbone was constructed by Zhu et al. [77]. Remarkably, this hybrid 1D
23 hierarchical structure showed significantly enhanced photocatalytic activity in H_2 production from
24 water splitting. Similarly, the work of Chava et al. [78] featured the development of 1D CdS–
25 Au/MoS₂ hierarchical core/shell heteronano structures (CSHNSs) by a facile two-step
26 hydrothermal method; high stability and efficiency toward hydrogens production were observed
27 with this nanophotocatalyst.

28 2D nanostructures, on the other hand, are desirable because they provide numerous reaction sites
29 due to their increased specific area. Their short diffusion length reduces the probability of
30 recombination of photoexcited charge carriers compared to the bulk forms of the photocatalysts

1 [68]. Ganguly et al. [70] provide a detailed review with emphasis on 2D nanomaterials for
 2 photocatalytic H₂ production. Zhang et al. [79] formulated a 2D nanophotocatalyst by doping
 3 ultrathin nanosheets of TiO₂ with quantum Cu(II) nanodots (QCNs). Their analysis further
 4 demonstrated that suppressing the recombination rate of the photogenerated electron-hole pair
 5 enhances the materials' photocatalytic performance. Xu et al. [80] showed that the photocatalytic
 6 activity of g-C₃N₄ nanosheets was improved by 13-fold after electrostatically assembling it with
 7 hematite α-Fe₂O₃ nanoplates. Pt was applied as a co-catalyst, whereas triethanolamine was utilized
 8 as a hole scavenger. A cost-effective and straightforward method for fabricating a hybrid 1D-2Dg-
 9 C₃N₄ heterojunction nanophotocatalyst has been proposed by Mahsoon et al. [68]. At present,
 10 modifications via co-catalysts for performance improvement, as shown in Fig. 2, have been
 11 exploited to enhance the catalytic performance [81].

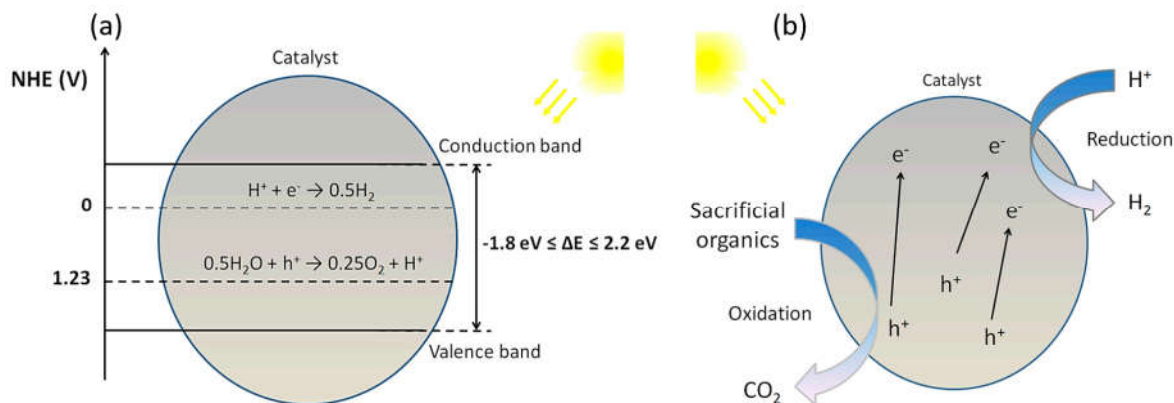


12
 13 **Figure 2:** (a) Pt co-catalyst appended to CdSe/CdS nanorods; (b,c) TEM images of CdSE/CdS
 14 nanorods showing Pt co-catalyst on one side; (d) Photocatalytic/photoelectrochemical H₂
 15 evolution for aqueous Na₂S solution; (e) H₂ evolution on CZTS-Pt nanoparticles. Adapted from
 16 Xu et al. [80], Khon et al. [82], Kalisman et al. [83], Moroz et al. [84], respectively.

1 Morphology adjustments, band edge repositioning, and surface structure alterations have also been
2 a subject of immense interest using these co-catalysts [66,85]. Their application may be carried
3 out in several forms, such as ion doping, noble metal doping, metal-ion implantation, and
4 sensitization [67,70]. Pt is the best noble metal for this purpose; however, its very high cost has
5 led to the application of alternative cheaper noble metals such as Ag, Ni, Ru, Cu, Pd, and Ir [67].
6 Sensitization, a promising strategy, involves using a sensitizer (nanosized-metal particles). The
7 sensitizer harvests sunlight (thus promoting visible light absorption), and thereafter, injects
8 electrons into the conduction band of the main photocatalyst –a process referred to as plasmon-
9 induced resonance energy transfer [64]. Furthermore, the tunable optical properties of
10 semiconductor polymer photocatalysts (usually achieved by altering the polymer building blocks)
11 has also gained research attention; poly(p-phenylene), poly(azomethine)s, polybenzothiadiazoles,
12 covalent organic frameworks, and microporous organic nanorods have been applied for
13 photocatalytic H₂ production [86]. Better light-harvesting efficiency may be attained with these
14 polymers when used with g-C₃N₄ compared to g-C₃N₄ alone [62].

15 Inorganic co-catalysts such as Ni-P have also been applied with pristine g-C₃N₄ to enhance their
16 photocatalytic activity [87]. The importance of this doping strategy has been effectively
17 demonstrated in the work of Kalisman et al. [83], where a record 100% photon to H₂ conversion
18 efficiency was attained using Pt-tipped CDSe@CdS nanophotocatalysts. However, the
19 photochemical instability of CdS and the high cost of Pt are the main limitations of this strategy
20 [83].

21 The application of metal oxide co-catalysts, which can act as photocatalysts themselves, has also
22 been demonstrated by Zada et al. [71]. SnO₂ as a metal oxide has an outstanding UV response,
23 although with a bandgap of 3.5eV. Its modifiable optical properties and exceptional stability make
24 it suitable for photocatalysis. The authors showed that the heterojunctional combination with g-
25 C₃N₄ with SnO₂ enhances charge separation for increased photocatalysis in comparison to g-C₃N₄
26 alone. For photocatalytic water splitting, Clarizia et al. [64] recommended that an efficient
27 photocatalyst should have a bandgap greater than 1.6–1.8 eV and should be narrower than 2.2eV
28 to allow efficient activation under natural solar irradiation. Fig.3 shows the required energy for
29 both solar driving and reforming photocatalytic reactions.



1
 2 **Figure 3:** (a) Required energy gap for solar-driven photocatalytic water splitting and (b)
 3 photocatalytic reforming of organic species. Reprinted from Clarizia et al. [64].
 4

5 Since photocatalytic reforming relies on the oxidation of organic sacrificial agents by
 6 photogenerated holes (which are in turn reduced by photogenerated electrons to form H₂ gas), it is
 7 required that the valence band be more positive than the redox potential of the sacrificial species,
 8 for efficient H₂ production [64]. Photoreforming of organics yields H₂ generation rates, which are
 9 more than 2 orders of magnitude higher than that of photocatalytic water splitting [88]. Hence,
 10 there is a need for an optimal selection of a sacrificial agent for these reactions. Further details of
 11 this photoreforming process can be found in the study of Clarizia et al. [64].

12 Biological systems, which are naturally nanoscaled, have also been employed as reliable platforms
 13 for engineering nanophotocatalysts. Photoelectrochemical analysis on TiO₂ catalyst shows
 14 effective charge transfer between a biological protein (bacteriorhodopsin) and TiO₂ nanoparticles
 15 and a consequent enhancement of photocatalytic ability (up to 5275 μmole of H₂ (μmole protein⁻¹
 16 h⁻¹) [72].

17 The discussion presented thus far demonstrates that a majority of the research efforts on the use of
 18 nanophotocatalysts for H₂ production have been mainly studied via experiments. Very few studies
 19 focusing on the application of theoretical/computational methods exist. These computational-
 20 based studies on nanophotocatalytic materials have mainly applied density functional theory
 21 (DFT) to predict ground-state properties as a function of the electronic density, primarily using
 22 TiO₂ photocatalysts. However, significant underestimations of the bandgap have been reported in
 23 many DFT-based studies [66]. The parameter is computed using the Kohn-Sham methods (via the
 24 generalized gradient approximation (GGA) or the local density approximation (LDA).

1 Nonetheless, using hybrid approaches, which utilized approximate DFT functionals (such as LDA)
2 with the exact Hartree-Fock method, can potentially improve computational accuracy. A summary
3 of some modelling-based studies in this regard is presented in Table 5.

Table 5: Summary of some recent research contributions on nanophotocatalytic generation of H₂.

Reference	Approach	Band gap information	Comments
Yu et al. [69]	Combination of hydrophilic polymers with a nanoprecipitation technique	— <i>However, a HOMO-LUMO gap is provided</i>	By applying a facile approach for the synthesis of nanoparticulate organic photocatalysts, a 70-fold improvement in the H ₂ evolution rate was obtained (37.2 mmol.h ⁻¹ .g ⁻¹) under sunlight irradiation.
Anthony Raja and Preethi. [89]	Experimental evaluation using a novel trapezoidal photoreactor	Reduction from 2.5 eV to 2.32 eV after CNT doping	Using synthesized CNT doped CdZnS/Fe ₂ O ₃ nano-photocatalyst, a H ₂ production rate of 2,679 μmol/h was obtained compared to CdZnS/Fe ₂ O ₃ only (2,009 μmol/h).
Zada et al. [71]	Robust experimental catalyst characterization	2.7 eV (g-C ₃ N ₄) and 3.5 eV (SnO ₂)	g-C ₃ N ₄ nanosheets were constructed and functionalized with SnO ₂ nanoparticles for H ₂ production from water splitting. The hybrid catalyst fabrication (g-C ₃ N ₄ – SnO ₂) enhanced H ₂ production compared to the individual application of g-C ₃ N ₄ and SnO ₂ .
Mahzoon et al. [68]	Novel synthesis method for (C ₃ N ₄ (1D-2D)) catalyst	2.70 (C ₃ N ₄ (1D)) 2.84 (C ₃ N ₄ (2D)) 2.78 (C ₃ N ₄ (1D-2D))	A method for the fabrication of 1D-2D g-C ₃ N ₄ heterojunction nanophotocatalyst was developed, which exhibited enhanced activity under visible light irradiation for H ₂ production (2.6 and 4.1 times that of C ₃ N ₄ (1D) and C ₃ N ₄ (2D), respectively).
Maghrabi et al. [90]	Simplex centroid design (SCD) and Box–Behnken design (BBD)	2.33 eV	Statistical optimal design of experiments was applied to fabricate a photocatalyst via optimal combinatorial ratios of α-MoO ₃ , WO ₃ and CdS catalysts. The produced catalyst showed high potential for H ₂ production from wastewater under a broad range of wavelengths.
Pati et al. [86]	Nanoprecipitation of polymer Pdots coupled with DFT validation	2.38 eV, 1.98 eV, and 2.46 eV for Pdots 1, 2 and 3, respectively	Converting an organic polymer into polymer nanoparticles via nanoprecipitation is an efficient way of significantly improving photocatalytic performance. An H ₂ evolution rate of up to 50 mmol.g ⁻¹ h ⁻¹ is achieved. N in the benzothiadiazole unit is the main reactive site.
Pavliuk et al. [81]	Experimental assessment using a photocatalytic reactor	—	A nano-hybrid assembly is produced by combining natural product stabilized Ag nanoparticles, TiO ₂ , and Ru nanoparticles as a co-catalyst. A solar-to-fuel efficiency of up to 20% was achieved compared to 10-12% efficiencies obtainable in conventional photovoltaic electrolysis.

Balasubramanian et al. [72]	H ₂ evolution measurements in a sealed reaction vessel	—	A light-harvesting biological proton pump (bacteriorhodopsin) was applied to enhance the visible light reactivity of TiO ₂ photocatalysts for photon reduction (to H ₂) using a Pt nanocrystalline catalyst.
Kaur and Singh. [91]	DFT calculations: 72-, 96- and 216-atom models utilized for amorphous TiO ₂ representation	2.85 eV, 2.85 eV & 2.7 eV for the 72-, 96- and 216-atom models	The electronic properties of amorphous and crystalline TiO ₂ for photocatalytic H ₂ production were compared. Amorphous TiO ₂ may be utilized as a cheaper, more abundant, but slightly less efficient photocatalyst than TiO ₂ in crystalline form.
Hanaor et al. [92]	Theoretical assessment using DFT	3 meV difference between the rutile and anatase phase	Cationic doping of TiO ₂ stabilizes the anatase phase relative to the rutile phase at standard conditions; anionic doping similarly inhibits anatase to rutile transformations. The effects of the tested dopants on the stability of the anatase phase are shown to be in the order: F>Si>Fe>Al
Das et al. [93]	Experimental assessment coupled with first-principles DFT calculations	—	The existence of charge transfer between graphene and deposited semiconductor and magnetic nanoparticles (TiO ₂ , ZnO, Fe ₃ O ₄ , Ni) was established. The possibility of tailoring the optoelectronic properties of graphene for H ₂ production was demonstrated.
Kanda et al. [94]	Experimental characterization of a metal chalcogenide.	Bulk value of 1.75 eV	A green and straightforward photodeposition technique was utilized for the coupling of MoS ₂ nanocrystals and MoO ₃ molecules with TiO ₂ . In HCOOH aqueous solutions, high photocatalytic activity of the MoS ₂ /TiO ₂ system is observed for H ₂ generation.

4.3 Nanomaterials for biological hydrogen production

Nanomaterials can be applied at different stages of biohydrogen production, including biomass pre-treatment, improved sugar and enzymes production, and enzymatic hydrolysis (Fig.4) [95].

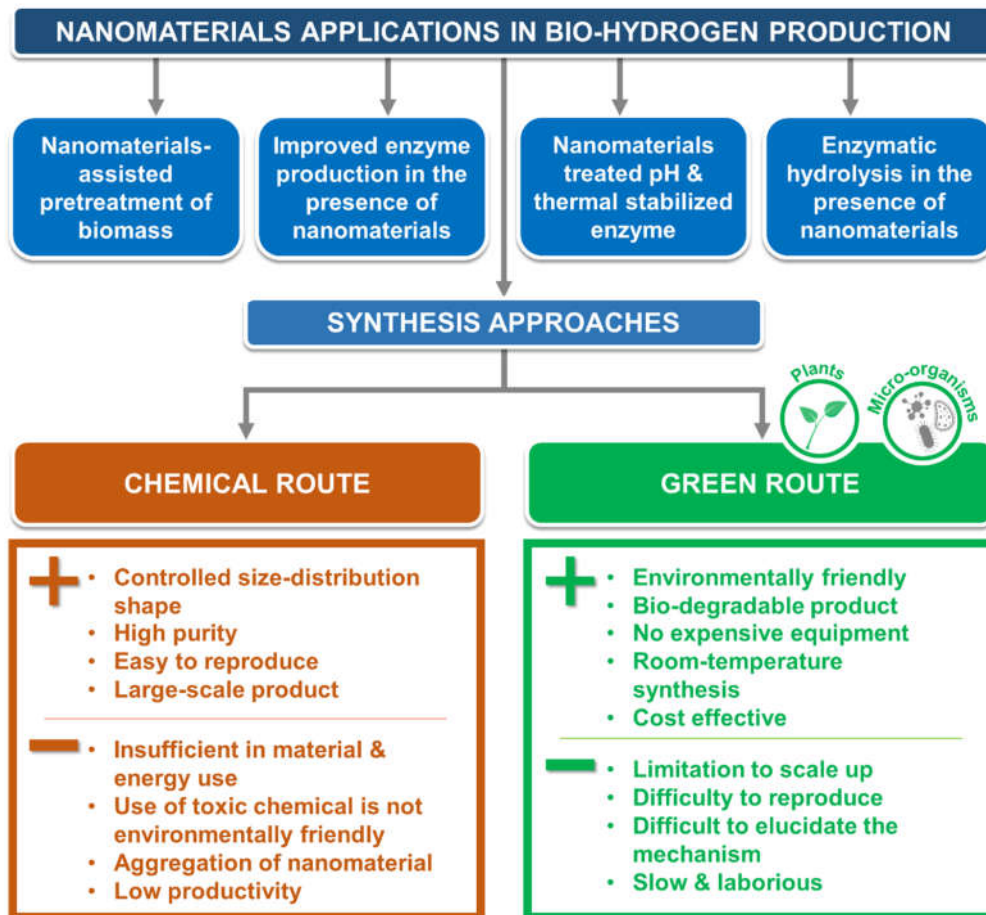


Figure 4: Application of nanomaterials at different stages of biological hydrogen production.

Nanomaterials such as Ni, Fe, and Cu play a significant role in improving biomass-to-biohydrogen processes. Fe and Ni behave like a cofactor on the active site of nitrogenase and hydrogenase enzymes, thereby elevating biohydrogen production yield [96]. They could also act as oxygen scavengers during fermentation by removing all the undesired oxygen present and minimizing the oxidation-reduction potential [95]. The removal of oxygen during fermentation creates a favourable anaerobic environment for the action of the hydrogenase enzyme and improves biohydrogen yield [97].

1 Previous studies also indicate that the addition of magnetic nanoparticles could influence the
2 thermal stability and pH of cellulase enzymes and reduce the lag phase of microorganisms leading
3 to improved hydrolysis [98]. In addition, the incorporation of magnetic nanoparticles (specifically
4 Fe and Ni) to the bioreactor can enhance hydrogen yield because of their ability to bond to the
5 active sites of the enzymes [99].

6 During dark fermentation, the hydrogenase enzymes are employed in breaking down sugar-rich
7 organic substrates in the absence of oxygen. Although dark fermentation produces improved
8 hydrogen yield, a low production rate is often observed [98]. Nanomaterials can create anoxic
9 conditions, permitting fast e^- transfer from e^- donors to the corresponding e^- acceptors, improving
10 reaction kinetics and biohydrogen yield [100].

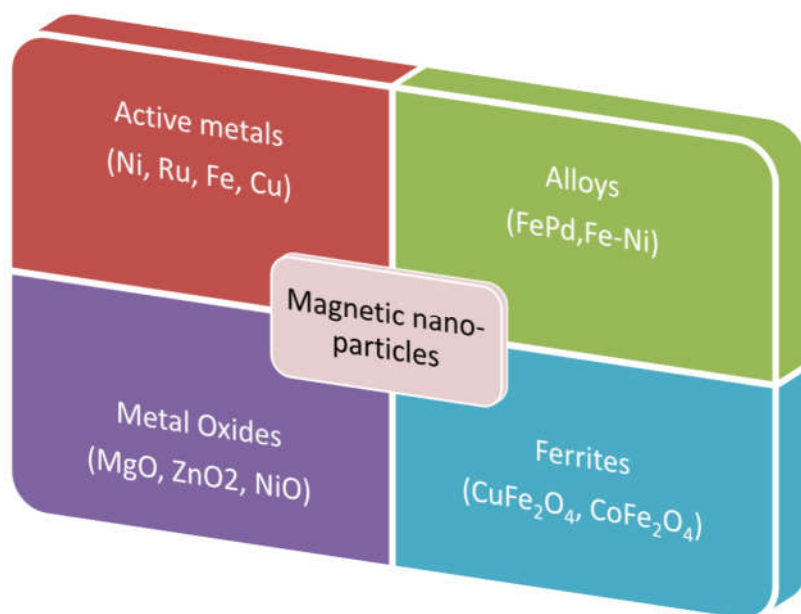
11 Engliman et al. [101] showed that the addition of Fe and Ni as metallic co-factors at the enzyme
12 active sites during fermentative hydrogen production could act as a biocatalyst towards improving
13 biohydrogen yield. The addition of Iron (II) oxide and nickel oxide under thermophilic conditions
14 of 60°C led to an increase in hydrogen yield by 34.38% and 5.47%, respectively, compared to the
15 control test [101]. Moreover, the microbes did not consume the metal nanoparticles at the end of
16 the experiments. Wang et al. [102] studied the effect of nickel nanomaterial addition on
17 biohydrogen production from dark fermentation. Optimal hydrogen production and biohydrogen
18 yield of 288.6 ml and 296.1 ml per g glucose consumed, respectively, were reported at 5 °C and
19 pH of 7.0 [102]. Taherdanak et al., [97]. used the central composite design (CCD) to study the
20 effect of Fe and Ni nanoparticles on biohydrogen production from dark fermentation. The addition
21 of both nanomaterials elevated the biohydrogen yield up to 200% higher than those in the
22 corresponding control test [97]. Studies have shown that nanomaterials have the potential to
23 modify the morphology of the microorganisms during dark fermentation in such a way that it could
24 lead to improved biohydrogen yield [103].

25 Nanomaterials could also be impactful in elevating the hydrogen yield of photo-fermentation
26 [104]. The nitrogenase enzymes used during photo-fermentation are dominated by Fe acting as a
27 major co-factor at the enzyme's active site [99]. Besides, the inclusion of Fe and Ni during photo-
28 fermentation helps maintain the enzymes' structural integrity. Moreover, photocatalytic
29 nanomaterials such as ZnO and TiO₂ can improve the photo-conversion efficiency of the bacteria
30 while supplying the required energy for hydrogen production [104]. The use of nanomaterials

1 during photo-fermentation also results in the fast transfer of a photo-induced electron to the
2 enzyme system, thereby improving the yield and productivity of hydrogen [104].

3 **4.4 Nanomaterials for thermochemical hydrogen production**

4 Nanomaterials are often used as active metals of heterogeneous catalysts or promoters during
5 thermochemical processes [105]. Specifically, Ni-based catalysts are promising for hydrothermal
6 gasification due to their small active metallic particle size, high dispersion rate, and effective
7 catalytic activity [106]. Other nanocatalysts used for thermochemical hydrogen production via
8 gasification include Fe, Cu, Pt, Ru, and Mg. The Ni nanocatalysts are preferred due to their low
9 cost and effective hydrogen selectivity in hydrothermal conditions. Magnetic nanoparticles for
10 thermochemical H₂ production can be classified as metal oxides, alloys, active metals, and ferrites,
11 as shown in Fig.5 [107].



12
13 **Figure 5:** Classification of different nanoparticles used as catalysts for thermochemical conversion
14 processes.

15 Fe–Ni supported on γ -Al₂O₃ showed improved catalysts ability during the gasification of algae
16 under hydrothermal conditions [106]. Zn nanoparticles were used as a promoter for Ru/ γ -Al₂O₃,
17 to improve H₂ yield during the hydrothermal gasification of bagasse. The addition of Zn
18 nanoparticles led to an elevation in the H₂ and total gas yield by 16.67% and 6.6%, respectively

1 [108]. Similarly, the addition of Cu promoter to Ni/CNT increased H₂ yield by a factor of 5.84
2 during the hydrothermal gasification of bagasse [109].

3 Metal oxide catalysts for thermochemical hydrogen production have been subjects of interest
4 among several researchers because of their stability, low price, and regeneration ability when
5 compared to transition metals catalysts [110]. Furthermore, the transition metal catalysts are prone
6 to sintering, agglomeration, and deactivation due to the harsh SCW conditions and not being cost-
7 efficient at large-scale applications. Metal oxides are easy to store, and transport and are more
8 stable than metal catalysts [111]. Different metal oxide catalysts that have been used for
9 thermochemical hydrogen production include WO₃, TiO₂, MgO, ZrO₂, ZnO, and NiO [111]. WO₃,
10 TiO₂, and ZrO₂ are effective in elevating the gasification efficiency of glucose under hydrothermal
11 conditions [111]. ZrO₂ and TiO₂ are widely known as thermally stable solid catalysts because of
12 their ability to prevent methanation reactions while promoting hydrogen production [110].

13 Nanoparticles, specifically Ni and Fe, can also be directly impregnated into biomass pores before
14 thermochemical conversion processes to eliminate the need for external heterogeneous catalysts
15 [112]. This technique showed promising hydrogen yield and gasification efficiency [112,113].

16 **5. Hydrogen storage methods**

17 As the efforts to maximize the potential of H₂ as a clean and efficient energy source intensify, its
18 efficient, safe and economical storage is critical for a thriving H₂ economy [114]. As a result of
19 this realization, H₂ storage technologies have gained the attention of researchers over time
20 [11,115,116]. Principally, H₂ is usually stored in four forms: compressed gas, liquefaction
21 (cryogenic), cryo-compressed, and solid-state storage. These various methods of storage are at
22 different stages of development. They have their strengths and weaknesses, making them apt for
23 various applications, as discussed in the following sections and summarized in Table 6.

24
25
26
27
28
29

1 **Table 6:** Pros and cons of different H₂ storage methods.

Hydrogen storage methods	Advantages	Limitations	References
Compressed gas	<ul style="list-style-type: none"> • Technology is matured and presently the best-understood method. • For underground storage, it is safer, saves space and can be stored for a long time • Lighter storage vessels are being developed. • H₂ is stored in its natural form and can be directly used when needed 	<ul style="list-style-type: none"> • Gravimetrically and volumetrically inefficient (low storage density) • High energy cost required to compress the gas • Large Storage vessels are required, leading to high space consumption, except in geological storage of compressed gas where gases are stored underground • Not suitable for long term storage (due to high pressure) except for geological storage • It is considered unsafe, as leakage may result in massive explosions 	Durbin and Malardier-Jugroot. [118] Peschel. [119]
Liquefaction	<ul style="list-style-type: none"> • Gravimetrically and volumetrically efficient (high storage density). • Technology is matured, hence developed. • Relatively smaller storage vessels are required. • Safer compared to compressed gas storage. 	<ul style="list-style-type: none"> • High energy is required for liquefaction. • Relatively high cost, mainly if carried out on a small scale. • Storage vessels are expensive and consume land space (relatively less than compression vessels). 	Durbin and Malardier-Jugroot. [118] Peschel. [119] Berstad et al.[120]
Solid-state-storage	<ul style="list-style-type: none"> • It is safer. • Large amounts of H₂ can be stored in small volumes at moderate temperatures and pressures. • It can store H₂ for a long time and relatively more conveniently. • It is highly efficient. 	<ul style="list-style-type: none"> • Regeneration is required before solid storage can be reused. • It can be expensive, especially for metal hydrides. • Regeneration is often slow. 	Abdalla et al. [11] Rusman and Dahari. [115] Zhevago et al. [116] Tarhan and Cil, [121]
Cyro-compressed	<ul style="list-style-type: none"> • It has more storage density than cryogenic storage. • It is a safe method of H₂ storage 	<ul style="list-style-type: none"> • High cost. • Lack of available infrastructure. 	Bhatt and Lee. [66] Moradi and

			Growth. [114]
--	--	--	------------------

1
2
3
4
5
6
7
8
9
10
11
12
13
14
15
16
17
18
19
20
21
22
23
24

5.1 Compressed gas storage

Compressed gas storage involves reducing the gas volume (while the pressure rises) to make it containable in a storage medium. Since H₂ has a relatively large volume for any given mass (due to its density), it is challenging to store it by compression. Moreover, its compression is energy-intensive and costly. For instance, the energy required to compress hydrogen gas to 600 bar is 20.48 MJ/Kg, while the energy needed for methane gas to 600 bar is 1.25 MJ/Kg. This difference is significant (more than 16 times higher) [124].

In compressed H₂ storage systems, the storage means and the compressor involved are integral parts of the system, as they significantly affect the system's safety, cost, and reliability. This section discusses two common storage means storage vessels and geological storage. H₂ can be stored in aquifers, depleted natural gas and oil reservoirs, salt caverns, abandoned mines, and rock caverns in geological storage. Among these, only the salt caverns have been explored so far. A detailed description of underground H₂ storage methodologies is presented elsewhere [122].

In contrast, storage vessels could either be at low pressure (0.95 MPa) or high pressure (>= 35 MPa) vessels [123]. Detailed information about H₂ storage in vessels can be found elsewhere [123]. Moreover, pressure vessels are made from various materials, and they are usually classified as Type I–V vessels [114,122,123]. Their properties are summarized in Table 7.

1 **Table 7:** Properties of pressure vessel types. Adapted from Elberry et al. [122], Moradi and
 2 Growth. [114], Ozaki et al. [123].

Pressure Vessel Type	Composition (-)	Density of storage vessel (kg_steel/m ³ _steel)	Relative cost (-)	Pressure Limit (MPa)
Type I	Metallic (carbon steel and low alloy steel)	1,360	Least expensive	50
Type II	Thick metallic hooped–wrapped composite (aluminum or steel and fibre resin)	816 to 952	50% more than Type I	No documented limit
Type III	Carbon fibre composite and aluminum (liner)	340 to 454	Double of Type II	45
Type IV	Polymer like HDPE (liner) and carbon fibre or carbon-glass composite	Very light	Very costly	100
Type V	Full composite (fibre reinforced shell)	20% lighter than Type IV	Very costly	Very limited (unfit for large-scale storage)

3

4 **5.2 Liquefaction/cryogenic storage**

5 Hydrogen can also be stored in liquid form at temperatures below 20 K, a method commonly
 6 referred to as cryogenic storage. In this form, the concentration of H₂ doubles that of compressed
 7 gas, leading to higher storage density and less storage volume. Few experimental studies have been
 8 published in this area over two decades [120].

9 As a result of this low boiling point (20 K), refrigeration, insulation, and vacuum superinsulation
 10 may be used to liquefy H₂ and maintain this liquid state [118,119,125]. For instance, refrigeration
 11 was successfully applied in the Ingolstadt and Leuna H₂ liquefaction plants to bring H₂ to 20 K
 12 temperature [126]. H₂ liquefaction in the Ingolstadt plant was carried out in four stages; two
 13 catalytic converters operating at isothermal conditions with liquid N₂ and liquid H₂ bath followed
 14 by two adiabatic steps. Bracha et al. [126] estimated the exergy efficiencies of the Ingolstadt and
 15 Leuna plants to be 21.0 and 23.6%, respectively. Modelling studies of large-scale plants have
 16 yielded up to 56.8% higher exergy efficiencies, with ortho-para conversion steps ranging from 2

1 stages to continuous technologies [120]. A detailed comparison of modelling and existing
2 liquefiers is presented elsewhere in the literature [120].

3 Although liquid H₂ storage is a matured technology with improved gravimetric and volumetric
4 efficiency, it still faces several challenges, including, but not limited to, high energy demand for
5 liquefaction, storage tank cost, heat transfer, and H₂ boil-off [114,125]. Between 35-40% of the
6 energy content in the stored H₂ is spent on liquefaction. This amount triples the energy required to
7 store the gas by compression [118]. As a result, H₂ liquefaction is capital intensive with its cost,
8 essentially dependent on the scale of production and plant location. About 60% of the capital
9 investment is attributable to equipment costs, 30% for infrastructure, and 10% for planning [125].
10 These highlighted challenges, among others, have hindered and limited the application of
11 cryogenic technology.

12 **5.3 Solid-state-storage**

13 H₂ can also be stored in solid-state, a more efficient method than the first two discussed because
14 the solid material can store relatively more significant quantities of H₂ in smaller volumes [121].
15 This can be done using nanostructured materials and hydrides, with the former having relatively
16 lower storage efficiencies, although with great potential. The latter can be classified into complex
17 hydrides, chemical hydrides, metal hydrides, and Magnesium-based alloys.

18 The potential of solid-state storage to meet the rising H₂ storage demand has attracted attention,
19 bringing it to the centre of recent H₂ storage discussions. Though most of the hydrides, like borate
20 hydrides of Na and Li, have high H₂ storage capacities, they face the problem of regeneration
21 efficiency and cost because most metals are expensive. Nitrides are promising due to the ease with
22 which they release H₂ when applied to solid-state H₂ storage. Chemical hydrides, which are
23 compounds of lighter elements than metals, have high storage capacity and easily decompose to
24 H₂. Magnesium-based alloys are light, cheap, readily available, and have increased storage
25 capacity but suffer from slow reaction rates even at high temperatures. This is currently a subject
26 of further research investigation and increasing the reaction rate [121].

27 Kumar et al. [127] designed a large-scale metal hydride-based H₂ storage system (MHHSS) and
28 studied the effect of supply pressure, temperature, and heat transfer fluid (HTF) flow rate on the
29 absorption and desorption rates of H₂. They found that as supply pressure increased, the mass of

1 H₂ absorbed and the absorption rate also increased. Chauhan et al. [128] conducted a study on the
2 uptake of H₂ by graphene nanoplatelets (GNP) at temperatures of 298K, 243K, and 99K and the
3 maximum adsorption was seen at 99K and 2 bar. This result agrees with that of Kumar et al. [127]
4 as both demonstrate the significant impact of temperature and pressure on adsorption and
5 desorption rates of H₂ gas. Another experiment conducted by Souahlia et al. [129] on metal
6 hydrides concluded that H₂ storage rates varied directly with the H₂ supply pressure. The cooling
7 temperature also has a marked impact on absorption, especially at low supply pressure.

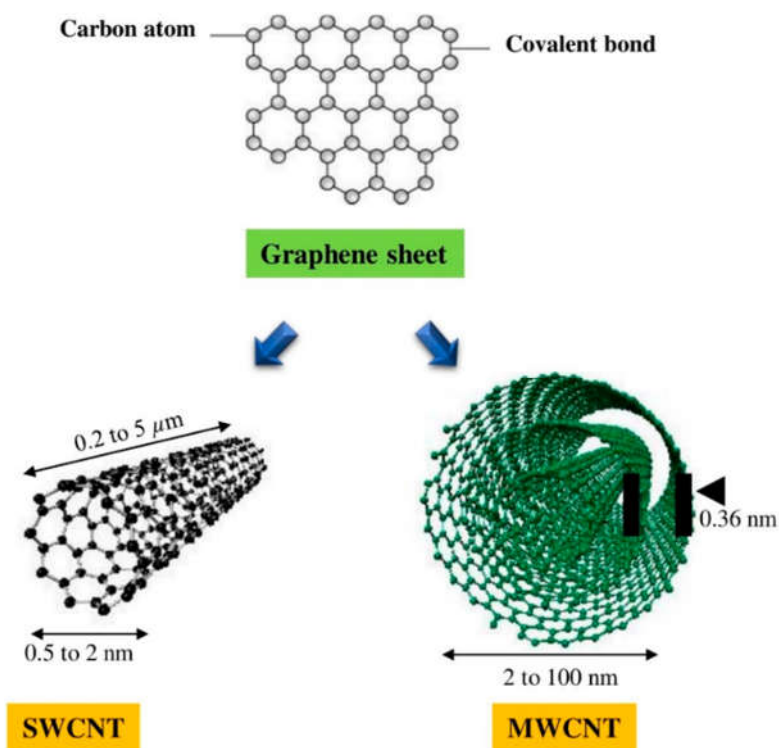
8 **5.4 Cyro-compressed H₂ gas storage**

9 This is a method of H₂ storage in which the gas is compressed in its supercritical state (~233°C).
10 At this stage, the gas cannot liquefy no matter how much it is compressed. This method produces
11 higher storage density than liquefied storage (about 10 g/L more than the liquefied storage) and is
12 safer [114]. Although promising, the Cyro-compressed hydrogen storage method currently lacks
13 the infrastructure for large-scale applications. A detailed discussion on this technology is outside
14 the scope of this review but outlined by Abdalla et al. [11] and Zhevago et al. [116].

15 **6. Nanomaterials for solid-state hydrogen storage**

16 **6.1 Carbon nanotubes**

17 Carbon nanotubes (CNT) are promising hydrogen storage materials due to their high adsorption
18 capacity at room temperatures, synthesizing simplicity from renewable feedstocks [130], along
19 with their highly microporous structure, chemical stability, and low mass density [131,132].
20 Carbon nanotubes, made of a graphene sheet rolled into a cylindrical tube shape, are categorized
21 as single-walled carbon nanotube (SWCNT) and multi-walled carbon nanotubes (MWCNT). The
22 SWCNT and MWCNT are characterized with an outer diameter range of 0.4 - 2 nm and 2 - 100
23 nm, respectively and 0.2-5 micron in length [133]. A conceptual diagram outlining the dimensions
24 of SWCNTs and MWCNTs is given in [Fig. 6](#).



1

2 **Figure 6.** Typical structure and dimensions of SWCNTs and MWCNTs. Reprinted from Patel et
 3 al. [134] with permission from Elsevier.

4 The electrical, thermal, mechanical characteristics of the SWCNT and MWCNT and production
 5 technologies are recently reported in detail by Patel et al. [134]. The structure, geometry, accessible
 6 surface area purity of the CNT, and the operating temperature and pressure, are the key factors
 7 affecting the hydrogen storage capacity [135]. Experimentally measured hydrogen storage
 8 capacities of different types of CNTs are given in Table 8.

9 **Table 8.** Hydrogen storage capacity of the various CNTs

	Hydrogen Storage (wt%)	Loading Temperature (K)	Loading Pressure (MPa)	References
CNT	9.6	77	10	Cheng et al. [130]
SWCNT	4.5	77	6	Panella et al. [136]
SWCNT	4.5	298	0.4	Mohan et al. [135]
MWCNT	6.3	298	14.8	Mohan et al. [135]
SWCNT (low purity)	5-10	406	0.04	Park and Keane. [137]

SWCNT (high purity)	8.25	80	7	Li et al. [138]
Aligned SWCNT	4	298	11	Chem et al. [139]
SWCNT	11.2	77	10	Dillon and Heben. [140]
Li-doped MWCNT	20	200-400	0.1	Dillon et al. [141]
K-doped MWCNT	14	300	0.1	Dillon et al. [141]
K-doped MWCNT	1.8	<313	0.1	Huang et al. [142]

1

2 The theoretical maximum hydrogen storage capacity of SWCNT was initially reported to be 5-10
3 wt% of CNT by Dillon et al. [143]. However, the possibility of reaching 11.2 wt% (Table 8) was
4 predicted and achieved in a study conducted by Dillon and Heben [140]. The increase in the carbon
5 storage capacity was attributed to arranging the carbon structure in a square lattice instead of a
6 hexagonal lattice and the operation conditions 77K and 10MPa [140]. However, hydrogen storage
7 at 77 K would not be feasible for onboard transportation on a commercial scale [132]. Therefore,
8 most research focuses on hydrogen storage at around ambient temperature (~278).

9 On the other hand, MWCNTs can achieve higher hydrogen storage due to their greater surface-
10 to-volume ratio. Their multi-layered nature allows the potential hydrogen uptake in between the
11 multiple graphene sheets [144]. However, the overall hydrogen storage capacity of the MWCNT
12 depends on operational conditions and the purity level, as the increased purity is directly linked to
13 the increased number of available sites for hydrogen adsorption [145]. Ioannatos et al. [145]
14 reported higher hydrogen storage capacities with higher purity CNTs when the operating
15 temperature was 298 K. The CNT synthesis methods and structural modifications play an essential
16 role. Mechanically bent CNTs are theoretically proven to have better thermodynamic properties
17 owing to their ΔH value of the adsorption process is being in the range of 20–50 kJ/mol H₂, in
18 comparison to the regular CNTs, which are likely to have thermodynamic dead end with a ΔH
19 smaller than zero or greater than 80 kJ/mol H₂ [146]. Similarly, cup-stacked carbon nanotubes
20 (CSCNT) have shown a 25% increase in hydrogen storage (has risen 1.13 w%) in comparison to
21 regular MWCNT [131].

1 **6.2 Carbon nanocomposites**

2 Carbon-based nanocomposites are multi-constituent materials with high specific areas and low-
3 cost processibility. Besides, they are highly attractive for solid-state hydrogen storage [147,148].
4 They exhibit excellent sorption kinetics due to their physicochemical attributes and facilitate low-
5 temperature desorption due to the presence of carbon as a metal-free dehydrogenation catalyst
6 [148–150].

7 Advanced concepts such as nanoconfinement, using suitably selected carbonaceous nano-
8 scaffold/nano-porous frameworks constitute promising routes for realizing reversible solid-state
9 hydrogen storage solutions [151,152]. Moreover, the presence of carbon can also enhance
10 desorption rates in nanocomposites by inhibiting the formation of undesirable ternary
11 intermediates, which can form during sorption and limit rehydrogenation (and invariably
12 reversibility) [149,153,154].

13 The inherent tailorability of the constituents of these nanocomposites renders them exceptionally
14 tuneable. Factors like pore size can play a significant role in tailoring the sorption/desorption
15 kinetics [154,155]. It has been shown by Sepehri et al. [156] that a reduction in pore size from 16
16 nm to 7 nm for carbon cryogel-ammonia borane nanocomposites results in a corresponding 20%
17 reduction in activation energy for desorption from 150 kJ/mol and up to 9% in peak
18 dehydrogenation temperatures. These trends are in agreement with those reported by Gross et al.
19 [151], who observed a 7% reduction in activation energy for desorption by decreasing pore size
20 by 48% in carbon-based LiBH₄ nanocomposites. Unsurprisingly, an increase in micro-pore volume
21 can yield better high-pressure and low-pressure hydrogen adsorption capacity for Nickel-activated
22 carbon nanocomposites [157].

23 It has been suggested that the viability of carbon-based nanoconfinement of light metal hydrides
24 for hydrogen storage applications depends significantly on the purity, functionality, and surface
25 properties of the carbon employed. These factors are believed to influence the reaction pathways
26 and thus, ultimately control desorption efficiency and reversibility. Comparing the reversibility of
27 carbon nanocomposites with high and low oxygen-based functionality on the carbon constituent,
28 Gao et al. [154] reported a reduction from 95% to 66% with successive rehydrogenation cycles.
29 Interestingly, despite reporting the presence of hydroxyl and carboxyl groups on the surface of
30 hexagonal mesoporous carbon frameworks used in their analysis, Li et al. [152] did not remark on

1 the possible effects of these oxygen-rich functional groups on the irreversibility of the carbon-
2 based ammonia borane nanocomposites investigated in their study. However, the authors did
3 highlight the beneficial effects of nanoconfinement in suppressing the evolution of volatiles, which
4 (owing to the risks of catalytic poisoning) precludes ammonia borane in hydrogen storage
5 applications.

6 The importance of the appropriate selection of the carbon constituent cannot be undermined. For
7 example, when combined with ammonia borane, carbon cryogels can suppress ammonia and
8 reduce dehydrogenation onset temperatures, whereas activated carbon can initiate room-
9 temperature dehydrogenation [158]. Another important consideration for using carbon
10 nanocomposites is that some carbon species can enhance sorption kinetics by reducing the
11 desorption temperature and participating in reversible hydrogen storage. This can be observed in
12 $\text{LiBH}_4\text{-C}_{60}$ nanocomposites where hydrogenation potential can be exploited with the lithium
13 borohydride and fullerene [150]. Table 9 summarizes some desorption characteristics of binary
14 and ternary carbon nanocomposites in recently published works.

Table 9: Comparative summary of sorption and desorption parameters reported in published literature.

Non-carbon constituents	Carbon-based constituent	Preparation methodology	^a W_c (%)	Pore size (nm)	Desorption capacity (wt%)	^b T_D (K)	^d $E_{a,D}$ (kJ/mol)	References
Mg–Nb@*	Amorphous carbon layer	Reactive gas evaporation	–	2**	4.8	573	59.7	Zhu et al. [159]
Mg(BH ₄) ₂ –*	Carbon aerogel	Melt infiltration	90	10	–	433	102	Yan et al. [149]
Mg–*	Carbon aerogel	Infiltration	77.5	19	2.15***	623	29.4	Liu et al. [160]
	Carbon aerogel						111	Gross et al. [151]
LiBH ₄ –*	Mesoporous carbon	Solution impregnation	67	4	3.4	573	–	Cahen et al. [161]
LiBH ₄ – Mg(BH ₄) ₂ –*	Activated carbon <i>IRH33</i>	Melt impregnation	72	<4	4	573	–	Zhao-Karger et al. [153]
AB–*	Carbon cryogel	Solution impregnation	76	2-50	9	358-383	120-150	Feaver et al. [155], Sepehri et al. [156]
	Lithium-doped mesoporous carbon <i>Li-CMK-3</i>	Solution impregnation & calcination	50	4.54	7	333	98	Li et al. [152]
	Graphene	High-energy ball milling	67	–	4.5	386	–	Bravo Diaz et al. [158]
	Activated carbon	High-energy ball milling	60	–	5.4	277	34	Bravo Diaz et al. [158]
	Activated carbon	Solution impregnation	60	–	5.4	285	–	Bravo Diaz et al. [158]

^a W_c : Weight fraction of carbon constituent (%); ^b T_D : Desorption temperature (K); ^c t_D : Desorption time at T_D (min); ^d $E_{a,D}$: Activation energy for desorption. The use of * denotes the carbon-based constituent; ** denotes a layer thickness; *** denotes a sorption capacity.

1 **6.3 Activated carbon**

2 Activated carbon (AC) is a physically or chemically modified form of carbon consisting of small
3 graphite crystallites and amorphous carbon with a specific surface area of 3000 m²/g. In physical
4 activation, the starting material is carbonized at high temperatures (700-1000°C) by steam or CO₂.
5 In contrast, chemical activation treats the starting materials (i.e., lignocellulosic biomass,
6 anthracite, coal precursor etc.) with chemicals such as H₃PO₄, KOH, NaOH, H₂SO₄, and ZnCl₂ at
7 500-800°C [162] [163]. It should be mentioned that ZnCl₂ is not a desirable activating agent due
8 to zinc emissions in the environment.

9 AC is suitable for both physisorption and hydrogen chemisorption due to its large surface area and
10 microporosity. However, choosing the right activating agent and precursor for the individual
11 applications is vital as these are the significant factors affecting the pore size and structure [164].
12 The KOH activation has been reported to be a particularly suitable method of hydrogen sorption
13 as it provides large surface areas, large pore volumes with a 1-2 nm uniform micropore size
14 distribution in the structure [144]. The result of the recent studies is given in Table 10.

15

1 **Table 10:** Hydrogen storage capacity of various AC

AC Precursor	Hydrogen Storage (wt%)	*S _{BET} (m ² /g)	Activating Agent	Loading Temperature (K)	Loading Pressure (MPa)	References
Pine lignin	1.61 1.93	1055 1409	CO ₂	11	0.1	Czarna-Juskiewicz et al. [165]
Coal from palm oil shell	0.29	640	KOH	268	0.4	Kapasiti et al. [166]
Coal from palm oil shell	6.7	3503	KOH	77	0.4	Zhao et al. [167]
Spent coffee beans	0.6 0.4	2070 2070	KOH	298 77	12 4	Akasaka et al. [168]
Anthracite	3.2 6.0 5.7 2.7	1149 2849 3220 1308	KOH/NaOH	77	4	Fierro et al. [169]
Carbon monolith	1.28	973	CO ₂	293	60	Series et al. [170]
Commercial AC	0.67 5.7	1060 3306	N/A	303 77	10 3	Xu et al. [171]
Anthracite	6.6	3441	KOH	77	4	Izquierdo and Celzard. [172]
Anthracite	5.5	2451	KOH/ Pd doped	298	8	Zhao et al. [173]

2 * BET (Brunauer-Emmett-Teller) analysis to measure the specific surface area available for adsorption.

3

4 The hydrogen storage capacity is mainly dependent on the specific surface area, the bulk density,
 5 and the loading temperature. Improved hydrogen storage capacities are achieved with the
 6 experiments conducted under cryogenic conditions with moderate pressure (1-10 MPa). In
 7 contrast, an average of 3 wt.% hydrogen sorption was seen in the experiments carried out at around
 8 room temperature due to the weak interaction between the adsorbate (H₂) and the adsorbent (AC)
 9 at room temperature. However, the reversible hydrogen storage capacity can be enhanced by

1 heteroatom doping as it dissociates the chemically bonded H₂ and subsequently allows the
2 diffusion of hydrogen atoms into the pores [144].

3 Chemical activation is another essential technique that impacts the hydrogen storage capacity as it
4 is directly linked to stimulation of micropores and correspondingly an increased adsorbent
5 porosity. The pore structure is also dependent on the activation temperature and the
6 KOH/precursor weight ratio. Furthermore, combined chemical and physical activation, using CO₂,
7 was reported to be effective in creating more micropores which resulted in an increased specific
8 surface area [165].

9 **6.4 Complex hydrides**

10 Complex metal hydrides (CMH) are a class of compounds with the general formula M(XH_n)_m,
11 where M usually represents a metal cation, whereas X is a metal or nonmetal element, which is
12 covalently bonded to hydrogen [174]. These compounds are hydrogen-rich and can be selectively
13 decomposed to produce H₂; thus, making complex hydrides of lightweight elements efficient H₂
14 storage media. Complex hydride hydrogen storage mechanism occurs as a two-stage process
15 involving dihydrogen dissociation into surface H atoms and the subsequent diffusion of the H
16 atoms into the bulk phase [175]. The many possible combinations of H₂ with elements like nitrogen
17 boron, oxygen, carbon, aluminum, and transition metals for CMH formation is an attribute that
18 allows functional property modification for H₂ storage purposes [176].

19 In comparison to other H₂ storage methods such as liquefaction, compression, and metal-organic
20 framework (MOF), CMHs have high H₂ density with the capability of de/rehydrogenation without
21 the requirements of very high pressures and low temperatures [177]. Ley et al. [178] reported that
22 only 0.034 m³ H₂ stored in δ-Mg(BH₄)₂ is required to power a family car for 500 km. This volume
23 is significantly smaller than the equivalent 60 m³ of H₂ required when standard fuel-cell-based
24 storage is applied at ambient temperature and pressure. This volumetric storage efficiency is one
25 of the factors that has led to extensive research contributions relating to the use of CMH for H₂
26 storage. However, their strong interaction with H₂ ($40 \leq \Delta H_{\text{ads}} \leq 100$ kJ/mol), very high desorption
27 temperatures (> 350 °C), irreversibility issues, slow kinetics, and challenging synthesis procedures
28 are formidable hindrances to their successful implementation [179]. For example, the thermal
29 decomposition of LiAlH₄ yields Li₃AlH₆ and Al, which is accompanied by an exothermic release

1 of H₂ gas. This initial exothermic decomposition has been shown to hinder the complete
2 reversibility of the system [176].

3 Research efforts targeted at mitigating these challenges have led to the development of several
4 thermodynamic and kinetic improvement strategies [175]. These include nanoconfinement via the
5 application of nanoporous hosts for interface contact improvement [180], catalytic modification
6 for enhancing H₂ sorption and desorption [181], and compositional alteration via anionic or
7 cationic substitution for composites formation in the CMH [182]. We present a discussion of past
8 contributions in light of these advancements while capturing the different classes of CMHs
9 (including alanates, borohydrides, amide-hydride composites, as well as metalorganic hydrides).

10 Alanates, a class of widely explored CMHs are generally composed of a metal cation and the
11 [AlH₄]⁻/[AlH₆]³⁻ anion, with storage capabilities of up to 10.4 wt.% (LiAlH₄), 9.3 wt.%
12 (Mg(AlH₄)₂) and 9.7 wt.% (LiMg(AlH₄)₃), respectively [175]. NaAlH₄ is the most extensively
13 studied alanate, given its relatively high gravimetric and volumetric H₂ densities, moderate heat of
14 de/rehydrogenation, and low cost of raw materials [183]. The successful application of NaAlH₄ as
15 H₂ storage material, when combined with catalysts such as nano-TiN to reduce the dissociation
16 temperature, instigated the search for other compatible metals [184]. Transition and rare earth
17 metals, such as Ti, Nb, Ce, Sm, Sc, have been applied via ball milling and wet doping methods to
18 reduce further the temperature required for the commencement of dehydrogenation [178,180].
19 Nanoparticles such as CeO₂, CeB₆, and CeFe₃ have been applied to improve the hydrogenation
20 duration of NaAlH₄ CMHs with timeframes as low as 20 mins observed [185]. The use of NaAlH₄
21 confined in carbon fibres has been reported to rapidly decrease the H₂ desorption temperature to
22 70 °C [186]. Similarly, NaAlH₄ confined in ordered mesoporous silica achieved dehydrogenation
23 within a temperature range of 125–150 °C [187]. Ti and TiO₂ nanoparticles embedded in
24 amorphous carbon have also shown promising potential for enhancing the H₂ storage capability of
25 NaAlH₄, with remarkable stability obtained after 100 adsorption/desorption cycles [188]. TiN
26 nanoparticles (nano-TiN@N-C) have also been demonstrated as reliable candidates for enhancing
27 the thermodynamics and kinetics of NaAlH₄ de/rehydrogenation [189,190]. Arora et al. [191]
28 employed DFT to explain the significant impact of experimental conditions (environmental
29 effects) on the thermodynamic stability (the free energy of formation) of metal-doped-NaAlH₄.
30 Similarly, DFT calculations implemented by Kang et al., [192] further verified the dependence

1 between the reaction energy and the chemical environmental conditions as well as the
2 morphological features.

3 Interest in metal borohydrides has been spurred by their very high H₂ contents and the existence
4 of a correlation between their experimentally determined decomposition temperature and the
5 metal's electronegativity (which strongly coordinates to the BH₄⁻ anionic groups) [178]. One of
6 the first studies to propose the use of metal borohydrides as an H₂ storage medium was that of
7 Zuttel et al. [193], achieving a H₂ capacity of up to 18.5 wt.%. Recently, the nanoconfinement of
8 Ca(BH₄)₂ and Mg(BH₄)₂ into porous hosts (Cu₂S) has been actively investigated; dehydrogenation
9 at 50 °C and full rehydrogenation at 300 °C were achieved [194]. The kinetic improvement of H₂
10 storage over M(BH₄)_m and M(NH₂BH₃)_m has been demonstrated using catalytic dopants (including
11 Fe₂O₃ and SiO₂) [195]. Bimetallic and trimetallic borohydrides and neutral molecule-modified
12 metal borohydrides (e.g. LiK(BH₄)₂, Li₃MgZn₅(BH₄)₁₅, Li₂Al(BH₄)₅·6NH₃), have also
13 demonstrated H₂ storage capabilities as documented by Møller et al. [176]. Nanoporous γ-
14 Mg(BH₄)₂ has been shown to efficiently store H₂ via adsorption onto the hydride's inner surface
15 and via chemical bonding to Boron [178]. Similarly, a study by Chen et al. [196] demonstrated
16 kinetic barrier reduction for enhancing the reversibility of Mg(BH₄)₂ using MgH₂ nanoparticles.
17 A recent study by Wood et al. [197] showed that mechanical stresses posed by an external
18 confining medium could affect the thermodynamics and kinetics of phase transformations that
19 occur during the de/rehydrogenation of some CMHs; they focused on incorporating more realistic
20 effects in their models which are usually neglected in computations based on ideal conditions.

21 Some unresolved challenges still plague the application of metal borohydrides for H₂ storage. The
22 exact mechanism of dehydrogenation and rehydrogenation of metal borohydrides is not well
23 understood (a possible consequence of the complex boron-hydrogen chemistry); furthermore, the
24 avoidance of effects such as diborane release, and the segregation of amorphous boron, are still
25 unresolved [178,193]. Moreover, alkali metal borohydrides possess higher stability (higher
26 decomposition temperatures > 350 °C) than alkali metal alanates (with decomposition
27 temperatures between 60 and 300 °C); on this basis, Møller et al. [176] reported that alkali metal
28 alanates might be better suited for H₂ storage applications.

29 As with the alanates, catalytic modification can be similarly pursued with amide hydrides using
30 transition metals, alkali metal hydrides, borohydrides, and other carbon-based materials [198].

1 However, these hydrides often portray very slow kinetics, which may be attributable to interface
2 reactions, diffusion processes, and nucleation [198]. Mechanical milling is an effective method,
3 which can be applied to mitigate this problem via grain size reduction and homogenization of the
4 amide and hydride particles [199]. This process has been applied to $K_2[Zn(NH_2)_4]$ as documented
5 in Cao et al. [198]. A further effect of this milling process is lowering the decomposition
6 temperature [176].

7 The presented discussion demonstrates a need to develop further methods for stabilizing H_2 storage
8 capacity at ambient conditions and particularly for long-term multiple usages. A primary safety
9 concern worth mentioning here relates to alanates, which have very high reactivity with water –
10 yielding large amounts of heat [174]. This exothermic hydrolysis reaction can initiate the hydride's
11 thermal decomposition in the case of accidental exposure to large amounts of water. Besides
12 storage capacity improvements, the operational safety of this H_2 storage technology is also worth
13 investigating further. Moreover, a comparison of different classes of CMHs is presented in Table
14 11.

15

1 **Table 11:** Comparison of the different classes of CMHs.

Class of CMH	Advantages	Limitations	References
Alanates	<ul style="list-style-type: none"> • Favourable dehydrogenation enthalpies • Rapid kinetics • Moderate H₂ capacities • Relatively easy preparation with readily available components 	<ul style="list-style-type: none"> • Insufficient reversible capacities for rehydrogenation • Contact with water is a safety concern 	Orimo et al. [174], He et al. [175]
Borohydrides	<ul style="list-style-type: none"> • High gravimetric H₂ capacities 	<ul style="list-style-type: none"> • Very slow kinetics • Side product formation (diborane) • Irreversibility • Poorly understood de/rehydrogenation mechanism 	Let et al. [178], Møller et al. [176] He et al. [175], Luo et al. [180]
Amide-Hydride	<ul style="list-style-type: none"> • Good thermodynamic stability • Moderate H₂ capacities 	<ul style="list-style-type: none"> • Very slow kinetics • Side product formation (mainly ammonia) 	Orimo et al. [174], He et al. [175]

2

3 **6.5 Metal-organic frameworks**

4 Metal-organic frameworks (MOFs), otherwise called porous coordination polymers, are a category
 5 of porous materials formed from metal ions or metal-containing nodes (secondary building units
 6 – mostly d-block transition metals) and organic linkers or multidentate ligands joined by
 7 coordinate bonds [200]. The available number of binding sites for these ligands at the metal centre
 8 often ranges from 2–12, yielding linear, cubic, octahedral, tetrahedral geometries [201]. An
 9 essential requirement in the selection of ligands for the development of porous MOFs is that the
 10 overall network be neutral. Otherwise, charged networks will cause the positioning of counter ions
 11 within the framework, which eventually reduces the porosity and H₂ storability of the framework
 12 material [202,203]. Unlike mesoporous oxide-based materials like zeolites, the structure and
 13 topology of the interior surface (of MOFs) on which H₂ is adsorbed can be easily modified for H₂
 14 storage enhancement (via metal selection and ligand functionalization) [204]. MOFs' modular
 15 construction and large surface areas and pore volumes allow for this modification [205].

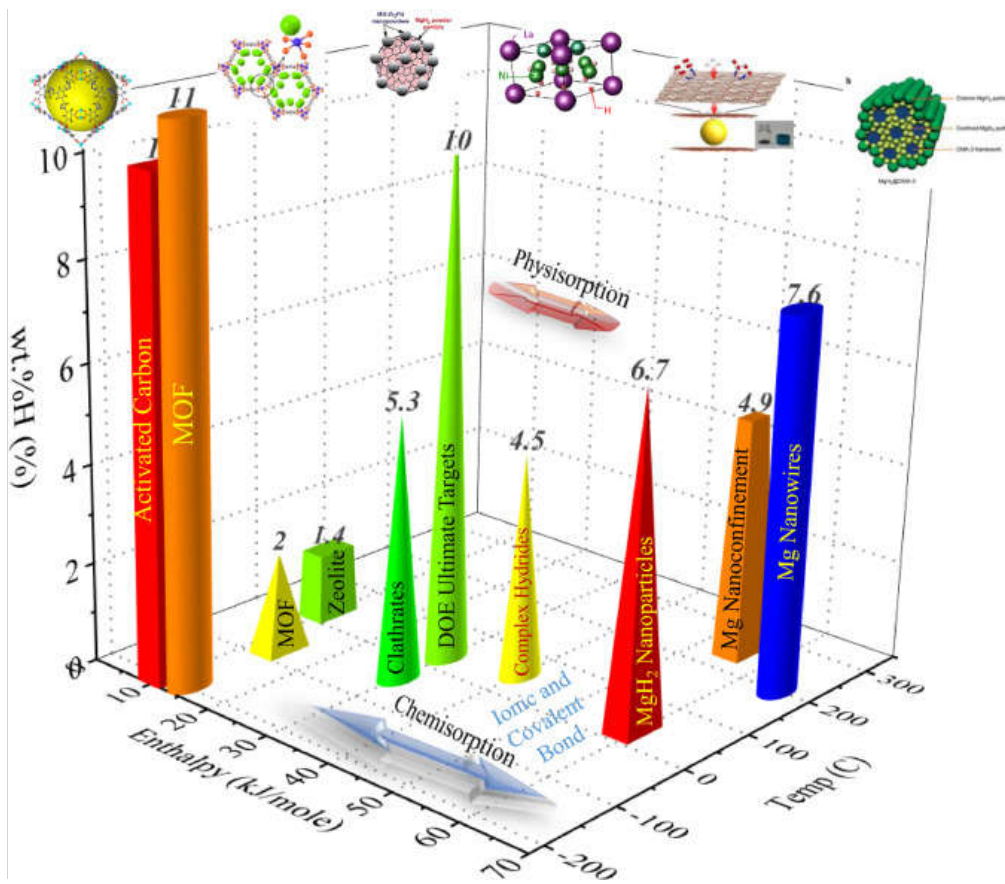
1 According to the ultimate target set by the US Department of Energy (DoE), onboard H₂ storage
2 systems should be able to achieve a gravimetric capacity of 6.5 wt.% (U.S Department of Energy,
3 2017). Although MOFs such as (MOF-5) have already surpassed the ultimate DoE targets (in terms
4 of gravimetric capacity) [207], sufficiently high surface area & pore volume and the formation of
5 viable (high-energy) H₂-binding sites (within the framework) are essential factors for the continual
6 development of other high-capacity MOFs, as well as their sustained cyclic performance. While
7 the first factor influences the H₂ uptake rate, the second influences the H₂-framework interaction.
8 Thus, the kinetics and thermodynamics of H₂ uptake and release must be accurately considered,
9 for effective H₂ storage capacity. MOFs can also potentially address the limitations of other
10 physisorbents (such as activated carbon and zeolites, which yield a similar H₂ uptake at low
11 temperatures but have reduced H₂ affinity at ambient temperatures) and chemical sorbents (e.g.,
12 hydrides, which possess reasonably high H₂ uptakes but poor release kinetics and
13 thermodynamics). Storage methods, which utilise chemical sorbents (like CMHs) particularly
14 suffer from the very tight binding of H₂ (ΔH_{ads} in the range of 50 to 200 kJ/mol); in contrast, the
15 ΔH_{ads} of physisorption techniques is minimal [208].

16 Isostructural metal-organic frameworks (IRMOF) based on Zn₄O are some of the widely studied
17 MOFs. The earliest demonstration of the H₂ storage capability of MOFs was reported by Yaghi et
18 al.[209]. Since this contribution, many MOFs have been studied with different H₂ storage
19 potentials [200]. These studies have applied several routes for increasing the H₂ uptake, e.g. surface
20 area and pore volume enhancement via increasing the ligand length, implementing mixed ligands,
21 and supercritical CO₂ drying [210,211]. More so, the use of multifunctional groups within the same
22 framework has also been demonstrated, with up to 84% improvement attained [212]. A summary
23 of some key methods of improving the H₂ uptake capacities of MOFs is presented in Table 12.

Table 12: Some applied methods for improving MOF performance.

Method	Comments	References
Sample preparation and activation via drying	Compared to traditional MOF pre-treatment methods (soaking samples in low boiling point solvents for porosity enhancement), freeze-drying and supercritical drying have been shown to improve pore performance significantly.	Ma et al. [213], Cooper and Rosseinsky. [214], Xiang et al. [215]
Unsaturated metal sites modification	These sites show significant H ₂ binding potential and are usually the first loading sites for H ₂ molecules. This depends on the cationic radius of the exposed metal site. Thermal-based activation has been applied to access the increased gas-adsorption potential of a MOF material.	Zhou et al. [216], Bagheri et al. [217]
Catenation/ Interpenetration	While this method increases the interaction between the framework and H atoms, it may also result in reduced pore volume, consequently reducing H ₂ storage. The effect of this method is also somewhat pressure-dependent.	Sule et al. [204], Zelenák and Saldan [202]
Functionalization of ligand structure	Covalent, coordinate, and covalent-coordinate modification are the primary enhancement routes. Aromatic substituents have shown promising potential for functionalizing ligand structures (due to additionally provided binding sites); thus, yielding improved H ₂ uptake compared to the pristine MOFs.	Rowsell et al. [218]
Chemical doping	This is a post-synthetic modification method using metals like cationic or atomic Lithium. As high as 7.5 times the storage capacity of the undoped IRMOF-14 has been reported using lithium. Doping with metal nanoparticles such as palladium nanoparticles is also a promising approach to achieving H ₂ storage at ambient conditions.	Mavrandonakis et al. [219], Cheng et al. [220]
Crystal size and morphology control	A strategy that enhances MOFs' poor volumetric packing/storage density has been presented in the literature. Packing density enhancement is achieved using the benchmark sorbent, MOF-5.	Suresh et al. [221]
Rapid evaluation of the surface area and pore volume	An empirical expression correlating the pore volume (V) or surface area (S) to the H ₂ uptake of selected MOFs allows the prediction of the sorption capacity of a new MOF using it V and S alone.	Kolotilov and Pavlishchuk. [222]

1 High storage capacities and rapid release kinetics have maintained MOFs at the forefront of
 2 established H₂ storage methodologies in light of the US Department of Energy (DoE) ultimate H₂
 3 storage targets. Increasing MOF-H₂ interactions at ambient temperatures and their volumetric
 4 packing efficiency are areas that will benefit from further investigations; thus, aiding the
 5 technological translation of this H₂ storage method. Fig.7 compares the performance of different
 6 H₂ storage materials with the DoE ultimate targets.



7
 8 **Figure 7:** Comparison of different H₂ storage materials. Reprinted from Gupta et al. [179] with
 9 permission from Elsevier.

10 6.6 Hydrogen storage in clathrates

11 Clathrate hydrates or hydrogen hydrates are compounds that incorporate guest molecules inside a
 12 host framework (polyhedral cages) comprising of H₂-bonded water molecules – on mixing water
 13 and H₂ gas at low temperatures, and high pressures, the guest molecules (H₂) are entrapped into
 14 the polyhedral cages of the host framework to form the hydrate [223]. Hydrogen bonding, van der
 15 Waals (dispersion) forces, and intermolecular interactions govern this process and are linked to

1 the structure's stability [224]. Without the encasement and corresponding support of these gas
 2 molecules, the structure of the hydrogen hydrates collapses into the water. Table 13 shows the
 3 structural properties of typical hydrate structures.

4 **Table 13:** Structure of commonly formed hydrogen hydrates Chattaraj et al. [225].

Type	Number of water molecules	Unit cell structure
sI	46	Two pentagonal dodecahedron (5^{12}) and six hexagonal truncated trapezohedron ($5^{12}6^2$) cages.
sII	136	Sixteen 5^{12} and eight $5^{12}6^4$ cages.
sH	36	Three 5^{12} , two $4^35^66^3$, and one $5^{12}6^8$ cages.

5
 6 A pioneering study by Mao et al. [226] demonstrated that pristine H₂ hydrates could store as high
 7 as 5 wt.% of H₂ at a pressure of 200 MPa and 243 K. This elevated pressure is a severe concern
 8 that limits its usage in mobile applications. One notable approach to mitigate this high-pressure
 9 requirement for H₂ hydrate formation is to develop binary hydrates which contain a helper
 10 molecule (gas or liquid) and H₂ as the second molecule. Further developments by Florusse et al.
 11 [227] involved the application of a water-soluble compound (THF) as an additive to significantly
 12 reduce the formation pressure to 5 MPa at 279.6 K; however, this caused a substantial drop in the
 13 H₂ storage capacity (1 wt.%).

14 Through the use of promoters such as THF, TBAB, and TBPB, Du et al. [228,229] formulated H₂
 15 hydrate at ambient pressure conditions. The effect of a simultaneous change in temperature and
 16 pressure has been shown to be favourable on the formation rate of H₂ hydrates (21% increase)
 17 while using a THF promoter [230]. Liu et al. [231] performed *ab initio* molecular dynamics
 18 simulations to investigate the impact of THF on H₂ storage capacity in clathrates and obtained
 19 capacities between 1.6 and 3.8 wt.% depending on THF concentration. Their computations also
 20 illustrated that a single H₂ molecule occupies the small cages of the hydrate, whereas the large
 21 cages are likely to contain one THF molecule together with one H₂ molecule. Ghaani et al. [232]
 22 utilized non-equilibrium molecular dynamics (NEMD) simulations to analyze H₂ release and
 23 uptake from propane planar clathrate surfaces at 180-273 K. The obtained experimental H₂ storage

1 capacity (using a fixed bed reactor) was 1.04 wt.% in comparison to the theoretically obtained 1.13
2 wt.% of the propane hydrate. A novel dual-function (thermodynamic and kinetic) promoter, 1,3-
3 dioxolane (DIOX), was proposed by Zhang et al. [233] for H₂-bearing sII hydrate formation.
4 Within 2 h, a H₂ uptake of up to 26.51 v/v (gas/hydrate) was attained, corresponding to a 30.2%
5 increase over the maximum H₂ uptake obtained using the conventional THF promoter. Besides the
6 above-mentioned promoters, other suggested promoters explored in the literature include tertiary
7 alcohols [234], argon [235], nitrogen [236], alkyl amines [237], methane [238], and SF₆ [239]. A
8 summary of important promoter molecules used in the past 20 years and their H₂ storage properties
9 is presented in Gupta et al. [179].

10 Despite the recent developments in enhancing the thermodynamics of H₂ hydrate storage
11 performance, formation and stabilization at moderate conditions, improving hydrate formation
12 kinetics is still a formidable challenge. The kinetics of hydrate formation in supercooled water-
13 hydrogen solution (without promoters) has been studied by del Rosso et al. [240] at 2000 bar and
14 263 K. It was postulated that the diffusion rate of H₂ limits the rate of hydrate formation through
15 the liquid phase. Immediately the transformation to solid is complete (after 18 h), the reaction rate
16 rapidly increases. The application of surfactants, nanoconfinements, and guest molecule
17 replacement (mainly via computational methodologies) are emerging research trends targeted at
18 resolving this problem of slow kinetics [241–243]. Recent developments by Di Profio et al. [244],
19 which apply a reverse micelles formation method, have shown significantly reduced time of H₂
20 hydrate formation (20 – 30 mins) using promoters like THF, THT, CP, and THT.

21 An important advantage of H₂ hydrate systems is the rapid and straightforward release of H₂. Thus,
22 no chemical reactions are needed for H₂ release since the binding energy is minimal
23 [224](Struzhkin et al., 2007). This eliminates the possibility of high dissociation heat requirements
24 as with metal hydrides. Stirring and the use of memory water (previously used water for hydrate
25 formation) have been investigated for further improving the release rate [230,241,242]. This
26 memory effect of water (during freezing and refreezing cycles) can be attributed to the occurrence
27 of microscopic hydrate residues in the water phase after low-temperature melting. These residues
28 subsequently act as nuclei for recrystallization during the hydrate formation phase, thus
29 accelerating the formation process [245]. One of the most recent studies [246], which
30 experimentally illustrated this memory effect, further confirmed this earlier proposed mechanism.

1 **7. Perspectives and future directions**

2 Nanomaterials have shown great promise in biological hydrogen production; however, the
3 mechanism of nanomaterial-influenced hydrogen production via biological routes is not well
4 understood. Moreover, the nanomaterial integrated approach for biological hydrogen production
5 is a study area that has not been explored. For instance, the combination of photo fermentation and
6 dark fermentation assisted with nanomaterials is an area that has not been explored. Integration of
7 different biological routes could provide new insights into the development of optimal and cost-
8 effective hydrogen production processes.

9 As far as nanoelectrocatalytic and nanophotocatalytic H₂ production is concerned, the
10 development of 2D nanomaterials with hybrid structures and multifunctional properties may
11 provide new opportunities to enhance their H₂ production potential via water splitting. Their large-
12 scale production in controlled environments is also worth investigating; however, this is dependent
13 on the novel research endeavours which provide insights into the complex catalytic mechanisms
14 rather than their catalytic performance for H₂ production alone.

15 Further research on the application of physisorbents materials (particularly activated carbon and
16 MOFs) for H₂ storage may focus on designing new functional materials with higher surface areas
17 and pore volumes, increased hydrostability, and sufficient interaction energy the retainment of H₂
18 at ambient temperatures. Furthermore, the application of carbon nanotubes for H₂ storage is
19 significantly affected by the purity and uncertainties governing their preparation. Further research
20 developments in this area may target robust synthesizing procedures that yield increased purity
21 and thus better H₂ storage capability. There is a need to study the effect of oxygen-rich carbon
22 groups on the reversibility of carbon-based nanocomposites; this is particularly important for
23 ammonia-borane variants. In addition, the identification of carbon-based nanomaterials that afford
24 the enhancement in adsorption kinetics and the ability to participate in the reversibility of hydrogen
25 storage is vital.

26 The hybrid application of earlier-discussed improvement strategies for CMHs (e.g.
27 nanoconfinement and catalytic doping) has strong potential to enhance their performance further
28 and requires further analysis. As earlier pointed out, the mechanisms of dehydrogenation and
29 rehydrogenation of some CMHs are not well understood (e.g., the mechanism of H₂ dissociation
30 and diffusion into and out of the bulk phase); this also increases the difficulty of distinguishing the

1 main mechanism of performance improvement when enhancement strategies are applied. These
2 strategies are also often associated with a high synthesis cost; more research endeavours are
3 required for simplification and cost reduction. The sensitivity of CMHs to air makes their
4 characterization difficult for H₂ storage analyses; thus, novel technologies are required for efficient
5 characterization. Accidental exposure of CMHs (particularly alanates) to large amounts of water
6 may instigate their thermal decomposition. Safety analyses of their large-scale application is also
7 worth investigating.

8 The presented discussion has summarized some of the challenges associated with H₂ hydrate
9 systems, including (extreme operating conditions in the absence of a promoter, slow formation
10 kinetics, low storage capacity, prolonged cyclic storage performance [uncertainties](#), [mass](#) transfer
11 constraints). However, the most significant of these challenges, limiting the application of this
12 technology for onboard storage, appears to be slow formation kinetics. Further developments are
13 particularly needed in this direction. In addition, H₂ hydrate formation appears to be mainly studied
14 using computational techniques; to enhance their accuracy via robust parameterization, more
15 experiments on the mechanism of H₂ hydrate crystallization are needed. The interaction of
16 additives has thus far been studied thermodynamically, further studies on the influence of molecule
17 migration may further improve the current understanding of their kinetics of formation.

18 Computational-based research on H₂ storage considering practical and rigorous conditions, and
19 accounting for practical uncertainties, need to be developed. Furthermore, a thorough economic
20 comparison of H₂ storage methods is still lacking in the literature. In addition, more studies are
21 required on the effect of industrial scaleup (particularly in terms of heat transfer) on larger samples
22 of these materials compared to the smaller samples usually applied in laboratory experiments.

23 The indirect storage of H₂ via its conversion to light hydrogen-containing chemicals such as formic
24 acid, methanol, methane and ammonia is also an area that requires future studies. These chemicals
25 are easy to store and transport and provide a carbon-free chemical energy carrier solution for the
26 transportation sector [247]. Ammonia storage, either in the liquid or gaseous form, is a mature
27 technology and has fewer challenges than hydrogen storage [248]. Furthermore, it is easier to
28 transport if ammonia is stored in the liquid form [247]. However, more studies are required in this
29 field, especially in process economics and life cycle assessment, to evaluate the economic
30 feasibility and environmental impacts of indirect hydrogen storage routes [249].

1 **8. Conclusions**

2 Nanomaterials are gaining more importance in addressing hydrogen production and storage
3 challenges. They can be applied in almost all technological breakthroughs, including catalysis,
4 metal-organic framework, complex hydrides, etc. This study outlines nanosized materials' specific
5 application to improve hydrogen production and storage. Specifically, nanomaterials are very
6 important in enhancing hydrogen yields of biological and thermochemical conversion processes.

7 Nanomaterials can be applied at different stages of biohydrogen production, including biomass
8 pre-treatment, improved sugar and enzymes production, and enzymatic hydrolysis. In contrast,
9 they can be used as catalysts and promoters during thermochemical processes. Nanomaterials
10 could also be impregnated directly to lignocellulosic biomass before thermochemical processes.
11 Ni and Fe are the most promising nanomaterials for H₂ production via thermochemical or
12 biological processes.

13 Several nanosized materials can be used for solid-state H₂ storage in the form of CNTs,
14 nanocomposites, AC, and MOF. All these materials have several advantages and limitations.
15 Although most of the hydrides, like borate hydrides of Na and Li, have high H₂ storage capacities,
16 they face the problem of regeneration efficiency and cost because most metals are expensive.

1 **References**

- 2 [1] Tian MW, Yuen HC, Yan SR, Huang WL. The multiple selections of fostering applications of
3 hydrogen energy by integrating economic and industrial evaluation of different regions. *Int J*
4 *Hydrogen Energy* 2019;44:29390–8. <https://doi.org/10.1016/j.ijhydene.2019.07.089>.
- 5 [2] Nanda S, Li K, Abatzoglou N, Dalai AK, Kozinski JA. Advancements and confinements in hydrogen
6 production technologies. *Bioenergy Syst Futur Prospect Biofuels Biohydrogen* 2017:373–418.
7 <https://doi.org/10.1016/B978-0-08-101031-0.00011-9>.
- 8 [3] Hydrogen Properties | Connecticut Hydrogen-Fuel Cell Coalition n.d. [http://chfcc.org/hydrogen-](http://chfcc.org/hydrogen-fuel-cells/about-hydrogen/hydrogen-properties/)
9 [fuel-cells/about-hydrogen/hydrogen-properties/](http://chfcc.org/hydrogen-fuel-cells/about-hydrogen/hydrogen-properties/) (accessed December 17, 2021).
- 10 [4] AFDC. Alternative Fuels Data Center: Hydrogen Benefits and Considerations.
11 *US_Department_of_Energy* 2017.
12 https://afdc.energy.gov/fuels/hydrogen_benefits.html
13 https://www.afdc.energy.gov/fuels/ethanol_benefits.html
14 https://www.afdc.energy.gov/fuels/hydrogen_benefits.html
15 <https://afdc.energy.gov/fuel> (accessed
December 17, 2021).
- 16 [5] Okolie JA, Patra BR, Mukherjee A, Nanda S, Dalai AK, Kozinski JA. Futuristic applications of
17 hydrogen in energy, biorefining, aerospace, pharmaceuticals and metallurgy. *Int J Hydrogen*
18 *Energy* 2021;46:8885–905. <https://doi.org/10.1016/j.ijhydene.2021.01.014>.
- 19 [6] Acar C, Dincer I. Comparative assessment of hydrogen production methods from renewable and
20 non-renewable sources. *Int J Hydrogen Energy* 2014;39:1–12.
21 <https://doi.org/10.1016/j.ijhydene.2013.10.060>.
- 22 [7] Boateng E, Chen A. Recent advances in nanomaterial-based solid-state hydrogen storage. *Mater*
23 *Today Adv* 2020;6:100022. <https://doi.org/10.1016/j.mtadv.2019.100022>.
- 24 [8] Liu W, Sun L, Li Z, Fujii M, Geng Y, Dong L, et al. Trends and future challenges in hydrogen
25 production and storage research. *Environ Sci Pollut Res* 2020;27:31092–104.
26 <https://doi.org/10.1007/s11356-020-09470-0>.
- 27 [9] Reddy NL, Rao VN, Vijayakumar M, Santhosh R, Anandan S, Karthik M, et al. A review on frontiers
28 in plasmonic nano-photocatalysts for hydrogen production. *Int J Hydrogen Energy*
29 2019;44:10453–72. <https://doi.org/10.1016/j.ijhydene.2019.02.120>.
- 30 [10] Mao SS, Shen S, Guo L. Nanomaterials for renewable hydrogen production, storage and
31 utilization. *Prog Nat Sci Mater Int* 2012;22:522–34. <https://doi.org/10.1016/j.pnsc.2012.12.003>.
- 32 [11] Abdalla AM, Hossain S, Nisfindy OB, Azad AT, Dawood M, Azad AK. Hydrogen production,
33 storage, transportation and key challenges with applications: A review. *Energy Convers Manag*
34 2018;165:602–27. <https://doi.org/10.1016/J.ENCONMAN.2018.03.088>.
- 35 [12] World Economic Forum. Grey, blue, green – the many colours of hydrogen explained | World
36 Economic Forum. 2021 7AD. [https://www.weforum.org/agenda/2021/07/clean-energy-green-](https://www.weforum.org/agenda/2021/07/clean-energy-green-hydrogen/)
37 [hydrogen/](https://www.weforum.org/agenda/2021/07/clean-energy-green-hydrogen/) (accessed December 15, 2021).
- 38 [13] Hydrogen: grey, blue, and BC green - Resource Works n.d.

- 1 <https://www.resourceworks.com/hydrogen-grey-blue> (accessed December 15, 2021).
- 2 [14] Nikolaidis P, Poullikkas A. A comparative overview of hydrogen production processes. *Renew*
3 *Sustain Energy Rev* 2017;67:597–611. <https://doi.org/10.1016/j.rser.2016.09.044>.
- 4 [15] Gunes B. A critical review on biofilm-based reactor systems for enhanced syngas fermentation
5 processes. *Renew Sustain Energy Rev* 2021;143:110950.
6 <https://doi.org/10.1016/j.rser.2021.110950>.
- 7 [16] Wang Q, Zhao Q, Wu RS, Tao XM, Zhang C. Review on copper- and palladium-based catalysts for
8 methanol steam reforming to produce hydrogen. *Xiandai Huagong/Modern Chem Ind*
9 2019;39:50–3. <https://doi.org/10.16606/j.cnki.issn0253-4320.2019.06.010>.
- 10 [17] Iulianelli A, Liguori S, Wilcox J, Basile A. Advances on methane steam reforming to produce
11 hydrogen through membrane reactors technology: A review. *Catal Rev - Sci Eng* 2016;58:1–35.
12 <https://doi.org/10.1080/01614940.2015.1099882>.
- 13 [18] Levin DB, Zhu H, Beland M, Cicek N, Holbein BE. Potential for hydrogen and methane production
14 from biomass residues in Canada. *Bioresour Technol* 2007;98:654–60.
15 <https://doi.org/10.1016/j.biortech.2006.02.027>.
- 16 [19] Kim Y, Kim M, Jeong H, Kim Y, Choi SH, Ham HC, et al. High purity hydrogen production via
17 aqueous phase reforming of xylose over small Pt nanoparticles on a γ -Al₂O₃ support. *Int J*
18 *Hydrogen Energy* 2020;45:13848–61. <https://doi.org/10.1016/j.ijhydene.2020.03.014>.
- 19 [20] El Doukkali M, Iriondo A, Arias PL, Requies J, Gandarías I, Jalowiecki-Duhamel L, et al. A
20 comparison of sol-gel and impregnated Pt or/and Ni based γ -alumina catalysts for bioglycerol
21 aqueous phase reforming. *Appl Catal B Environ* 2012;125:516–29.
22 <https://doi.org/10.1016/j.apcatb.2012.06.024>.
- 23 [21] Zoppi G, Pipitone G, Gruber H, Weber G, Reichhold A, Pirone R, et al. Aqueous phase reforming of
24 pilot-scale Fischer-Tropsch water effluent for sustainable hydrogen production. *Catal Today*
25 2021;367:239–47. <https://doi.org/10.1016/j.cattod.2020.04.024>.
- 26 [22] Freni S, Calogero G, Cavallaro S. Hydrogen production from methane through catalytic partial
27 oxidation reactions. *J Power Sources* 2000;87:28–38. [https://doi.org/10.1016/S0378-](https://doi.org/10.1016/S0378-7753(99)00357-2)
28 [7753\(99\)00357-2](https://doi.org/10.1016/S0378-7753(99)00357-2).
- 29 [23] Okolie JA, Nanda S, Dalai AK, Berruti F, Kozinski JA. A review on subcritical and supercritical water
30 gasification of biogenic, polymeric and petroleum wastes to hydrogen-rich synthesis gas. *Renew*
31 *Sustain Energy Rev* 2020;119:109546. <https://doi.org/10.1016/j.rser.2019.109546>.
- 32 [24] Demirbaş A. Biomass resource facilities and biomass conversion processing for fuels and
33 chemicals. *Energy Convers Manag* 2001;42:1357–78. [https://doi.org/10.1016/S0196-](https://doi.org/10.1016/S0196-8904(00)00137-0)
34 [8904\(00\)00137-0](https://doi.org/10.1016/S0196-8904(00)00137-0).
- 35 [25] Demirbaş A. Yields of hydrogen-rich gaseous products via pyrolysis from selected biomass
36 samples. *Fuel* 2001;80:1885–91. [https://doi.org/10.1016/S0016-2361\(01\)00070-9](https://doi.org/10.1016/S0016-2361(01)00070-9).
- 37 [26] Duman G, Uddin MA, Yanik J. Hydrogen production from algal biomass via steam gasification.
38 *Bioresour Technol* 2014;166:24–30. <https://doi.org/10.1016/j.biortech.2014.04.096>.

- 1 [27] Iribarren D, Susmozas A, Petrakopoulou F, Dufour J. Environmental and exergetic evaluation of
2 hydrogen production via lignocellulosic biomass gasification. *J Clean Prod* 2014;69:165–75.
3 <https://doi.org/10.1016/j.jclepro.2014.01.068>.
- 4 [28] Wang Z, He T, Qin J, Wu J, Li J, Zi Z, et al. Gasification of biomass with oxygen-enriched air in a
5 pilot scale two-stage gasifier. *Fuel* 2015;150:386–93. <https://doi.org/10.1016/j.fuel.2015.02.056>.
- 6 [29] Fremaux S, Beheshti SM, Ghassemi H, Shahsavan-Markadeh R. An experimental study on
7 hydrogen-rich gas production via steam gasification of biomass in a research-scale fluidized bed.
8 *Energy Convers Manag* 2015;91:427–32. <https://doi.org/10.1016/j.enconman.2014.12.048>.
- 9 [30] Okolie JA, Rana R, Nanda S, Dalai AK, Kozinski JA. Supercritical water gasification of biomass: A
10 state-of-the-art review of process parameters, reaction mechanisms and catalysis. *Sustain Energy*
11 *Fuels* 2019;3:578–98. <https://doi.org/10.1039/c8se00565f>.
- 12 [31] Ahmad AA, Zawawi NA, Kasim FH, Inayat A, Khasri A. Assessing the gasification performance of
13 biomass: A review on biomass gasification process conditions, optimization and economic
14 evaluation. *Renew Sustain Energy Rev* 2016;53:1333–47.
15 <https://doi.org/10.1016/j.rser.2015.09.030>.
- 16 [32] Kruse A. Hydrothermal biomass gasification. *J Supercrit Fluids* 2009;47:391–9.
17 <https://doi.org/10.1016/j.supflu.2008.10.009>.
- 18 [33] Adar E, Ince M, Karatop B, Bilgili MS. The risk analysis by failure mode and effect analysis (FMEA)
19 and fuzzy-FMEA of supercritical water gasification system used in the sewage sludge treatment. *J*
20 *Environ Chem Eng* 2017;5:1261–8. <https://doi.org/10.1016/j.jece.2017.02.006>.
- 21 [34] Rodriguez Correa C, Kruse A. Supercritical water gasification of biomass for hydrogen production
22 – Review. *J Supercrit Fluids* 2018;133:573–90. <https://doi.org/10.1016/j.supflu.2017.09.019>.
- 23 [35] Das D, Veziroğlu TN. Hydrogen production by biological processes: A survey of literature. *Int J*
24 *Hydrogen Energy* 2001;26:13–28. [https://doi.org/10.1016/S0360-3199\(00\)00058-6](https://doi.org/10.1016/S0360-3199(00)00058-6).
- 25 [36] Kapdan IK, Kargi F. Bio-hydrogen production from waste materials. *Enzyme Microb Technol*
26 2006;38:569–82. <https://doi.org/10.1016/j.enzmictec.2005.09.015>.
- 27 [37] Ni M, Leung DYC, Leung MKH, Sumathy K. An overview of hydrogen production from biomass.
28 *Fuel Process Technol* 2006;87:461–72. <https://doi.org/10.1016/j.fuproc.2005.11.003>.
- 29 [38] Holladay JD, Hu J, King DL, Wang Y. An overview of hydrogen production technologies. *Catal*
30 *Today* 2009;139:244–60. <https://doi.org/10.1016/j.cattod.2008.08.039>.
- 31 [39] Das D, Veziroglu TN. Advances in biological hydrogen production processes. *Int J Hydrogen*
32 *Energy* 2008;33:6046–57. <https://doi.org/10.1016/j.ijhydene.2008.07.098>.
- 33 [40] Herbaut M, Sijaj M, Claverie JP. Nanomaterials-Based Water Splitting: How Far Are We from a
34 Sustainable Solution? *ACS Appl Nano Mater* 2021;4:907–10.
35 <https://doi.org/10.1021/acsnm.1c00246>.
- 36 [41] Safari F, Dincer I. A review and comparative evaluation of thermochemical water splitting cycles
37 for hydrogen production. *Energy Convers Manag* 2020;205:112182.

- 1 <https://doi.org/10.1016/J.ENCONMAN.2019.112182>.
- 2 [42] MarcelloDe Falco LMG laquaniello. Membrane reactors for hydrogen production processes.
3 London, England: Springer; 2011. <https://doi.org/10.1007/978-0-85729-151-6> Springer.
- 4 [43] McKendry P. Energy production from biomass (part 1): Overview of biomass. *Bioresour Technol*
5 2002;83:37–46. [https://doi.org/10.1016/S0960-8524\(01\)00118-3](https://doi.org/10.1016/S0960-8524(01)00118-3).
- 6 [44] Levene JI, Mann MK, Margolis RM, Milbrandt A. An analysis of hydrogen production from
7 renewable electricity sources. *Sol Energy* 2007;81:773–80.
8 <https://doi.org/10.1016/j.solener.2006.10.005>.
- 9 [45] Bak T, Nowotny J, Rekas M, Sorrell CC. Photo-electrochemical properties of the TiO₂-Pt system in
10 aqueous solutions. *Int J Hydrogen Energy* 2002;27:19–26. [https://doi.org/10.1016/S0360-3199\(01\)00090-8](https://doi.org/10.1016/S0360-3199(01)00090-8).
- 11
- 12 [46] Cao LM, Lu D, Zhong DC, Lu TB. Prussian blue analogues and their derived nanomaterials for
13 electrocatalytic water splitting. *Coord Chem Rev* 2020;407:213156.
14 <https://doi.org/10.1016/j.ccr.2019.213156>.
- 15 [47] energy.org. Hydrogen Production: Photoelectrochemical Water Splitting | Department of Energy
16 2020. [https://www.energy.gov/eere/fuelcells/hydrogen-production-photoelectrochemical-
17 water-splitting](https://www.energy.gov/eere/fuelcells/hydrogen-production-photoelectrochemical-water-splitting) (accessed August 11, 2021).
- 18 [48] Song W, Li M, Wang C, Lu X. Electronic modulation and interface engineering of electrospun
19 nanomaterials-based electrocatalysts toward water splitting. *Carbon Energy* 2021;3:101–28.
20 <https://doi.org/10.1002/cey2.85>.
- 21 [49] Narwade SS, Mali SM, Digraskar R V., Sapner VS, Sathe BR. Ni/NiO@rGO as an efficient
22 bifunctional electrocatalyst for enhanced overall water splitting reactions. *Int J Hydrogen Energy*
23 2019;44:27001–9. <https://doi.org/10.1016/j.ijhydene.2019.08.147>.
- 24 [50] Paul SC, Dey SC, Molla MAI, Islam MS, Debnath S, Miah MY, et al. Nanomaterials as
25 electrocatalyst for hydrogen and oxygen evolution reaction: Exploitation of challenges and
26 current progressions. *Polyhedron* 2021;193:114871. <https://doi.org/10.1016/j.poly.2020.114871>.
- 27 [51] Kumar S, Srivastava R, Chattopadhyay J. MxOy/M/graphene coated multi-shelled nano-sphere as
28 Bi-functional electrocatalysts for hydrogen and oxygen evolution. *Int J Hydrogen Energy*
29 2021;46:341–56. <https://doi.org/10.1016/j.ijhydene.2020.09.139>.
- 30 [52] Wang B, Zhou Y, Hou Q, Han Y, Huo W, Luo T, et al. One stable electrocatalyst for two evolution
31 reactions by one-pot combustion synthesis. *Int J Hydrogen Energy* 2020;45:22691–9.
32 <https://doi.org/10.1016/j.ijhydene.2020.06.077>.
- 33 [53] Wan S, Hu J, Li GD, Yang L, Liu Y, Gao R, et al. Nano-netlike carbon fibers decorated with highly
34 dispersed CoSe₂nanoparticles as efficient hydrogen evolution electrocatalysts. *J Alloys Compd*
35 2017;702:611–8. <https://doi.org/10.1016/j.jallcom.2017.01.207>.
- 36 [54] Han HS, Yi F, Choi S, Kim J, Kwon J, Park K, et al. Self-supported vanadium-incorporated cobalt
37 phosphide as a highly efficient bifunctional electrocatalyst for water splitting. *J Alloys Compd*
38 2020;846:156350. <https://doi.org/10.1016/j.jallcom.2020.156350>.

- 1 [55] Jadhav RG, Singh D, Krivoschapkin P V., Das AK. Electrodeposited Organic-Inorganic Nanohybrid as
2 Robust Bifunctional Electrocatalyst for Water Splitting. *Inorg Chem* 2020;59:7469–78.
3 <https://doi.org/10.1021/acs.inorgchem.0c00227>.
- 4 [56] Yan Q, Chen X, Wei T, Wang G, Zhu M, Zhuo Y, et al. Hierarchical Edge-Rich Nickel Phosphide
5 Nanosheet Arrays as Efficient Electrocatalysts toward Hydrogen Evolution in Both Alkaline and
6 Acidic Conditions. *ACS Sustain Chem Eng* 2019;7:7804–11.
7 <https://doi.org/10.1021/acssuschemeng.8b06861>.
- 8 [57] Dai W, Ren K, Zhu Y an, Pan Y, Yu J, Lu T. Flower-like CoNi₂S₄/Ni₃S₂ nanosheet clusters on nickel
9 foam as bifunctional electrocatalyst for overall water splitting. *J Alloys Compd* 2020;844:156252.
10 <https://doi.org/10.1016/j.jallcom.2020.156252>.
- 11 [58] Kumar A, Bhattacharyya S. Porous NiFe-Oxide Nanocubes as Bifunctional Electrocatalysts for
12 Efficient Water-Splitting. *ACS Appl Mater Interfaces* 2017;9:41906–15.
13 <https://doi.org/10.1021/acsami.7b14096>.
- 14 [59] Zeng L, Sun K, Wang X, Liu Y, Pan Y, Liu Z, et al. Three-dimensional-networked Ni₂P/Ni₃S₂
15 heteronanoflake arrays for highly enhanced electrochemical overall-water-splitting activity. *Nano*
16 *Energy* 2018;51:26–36. <https://doi.org/10.1016/j.nanoen.2018.06.048>.
- 17 [60] Mugheri AQ, Daudpoto MR, Mugheri AA, Kalhoro DM. Recent progress in doping-induced
18 structural and electronic modification in Cu–SnCo interconnected network enhanced efficient
19 performance evidence for the hydrogen evolution reaction: current state and prospects. *J Porous*
20 *Mater* 2021;1:1–10. <https://doi.org/10.1007/s10934-021-01084-2>.
- 21 [61] Wang C, Zhang P, Lei J, Dong W, Wang J. Integrated 3D MoSe₂@Ni_{0.85}Se Nanowire Network
22 with Synergistic Cooperation as Highly Efficient Electrocatalysts for Hydrogen Evolution Reaction
23 in Alkaline Medium. *Electrochim Acta* 2017;246:712–9.
24 <https://doi.org/10.1016/j.electacta.2017.06.028>.
- 25 [62] Wang L, Fernández-Terán R, Zhang L, Fernandes DLA, Tian L, Chen H, et al. Organic Polymer Dots
26 as Photocatalysts for Visible Light-Driven Hydrogen Generation. *Angew Chemie* 2016;128:12494–
27 8. <https://doi.org/10.1002/ange.201607018>.
- 28 [63] Qian W, Xu S, Zhang X, Li C, Yang W, Bowen CR, et al. Differences and Similarities of
29 Photocatalysis and Electrocatalysis in Two-Dimensional Nanomaterials: Strategies, Traps,
30 Applications and Challenges. *Nano-Micro Lett* 2021;13:1–38. <https://doi.org/10.1007/s40820-021-00681-9>.
- 32 [64] Clarizia L, Russo D, Di Somma I, Andreozzi R, Marotta R. Hydrogen generation through solar
33 photocatalytic processes: A review of the configuration and the properties of effective metal-
34 based semiconductor nanomaterials. *Energies* 2017;10. <https://doi.org/10.3390/en10101624>.
- 35 [65] Puga A V. Photocatalytic production of hydrogen from biomass-derived feedstocks. *Coord Chem*
36 *Rev* 2016;315:1–66. <https://doi.org/10.1016/j.ccr.2015.12.009>.
- 37 [66] Bhatt MD, Lee JS. Nanomaterials for photocatalytic hydrogen production: From theoretical
38 perspectives. *RSC Adv* 2017;7:34875–85. <https://doi.org/10.1039/c7ra03435k>.
- 39 [67] Kumar R, Suyamburajan VA, Khan A, Asiri AM, Dzudzevic-Cancar H. Nanophotocatalysts for

- 1 hydrogen production applications. *Nanomater Hydrog Storage Appl* 2021;219–29.
2 <https://doi.org/10.1016/b978-0-12-819476-8.00018-9>.
- 3 [68] Mahzoon S, Nowee SM, Haghghi M. Synergetic combination of 1D-2D g-C3N4 heterojunction
4 nanophotocatalyst for hydrogen production via water splitting under visible light irradiation.
5 *Renew Energy* 2018;127:433–43. <https://doi.org/10.1016/j.renene.2018.04.076>.
- 6 [69] Yu M, Zhang W, Guo Z, Wu Y, Zhu W. Engineering Nanoparticulate Organic Photocatalysts via a
7 Scalable Flash Nanoprecipitation Process for Efficient Hydrogen Production. *Angew Chemie - Int*
8 *Ed* 2021;60:15590–7. <https://doi.org/10.1002/anie.202104233>.
- 9 [70] Ganguly P, Harb M, Cao Z, Cavallo L, Breen A, Dervin S, et al. 2D Nanomaterials for Photocatalytic
10 Hydrogen Production. *ACS Energy Lett* 2019;4:1687–709.
11 <https://doi.org/10.1021/acscenergylett.9b00940>.
- 12 [71] Zada A, Khan M, Qureshi MN, Liu SY, Wang R. Accelerating Photocatalytic Hydrogen Production
13 and Pollutant Degradation by Functionalizing g-C3N4 With SnO2. *Front Chem* 2020;7:941.
14 <https://doi.org/10.3389/fchem.2019.00941>.
- 15 [72] Balasubramanian S, Wang P, Schaller RD, Rajh T, Rozhkova EA. High-performance bioassisted
16 nanophotocatalyst for hydrogen production. *Nano Lett* 2013;13:3365–71.
17 <https://doi.org/10.1021/nl4016655>.
- 18 [73] Li X, Hou Y, Zhao Q, Teng W, Hu X, Chen G. Capability of novel ZnFe2O4 nanotube arrays for
19 visible-light induced degradation of 4-chlorophenol. *Chemosphere* 2011;82:581–6.
20 <https://doi.org/10.1016/j.chemosphere.2010.09.068>.
- 21 [74] Pachfule P, Acharjya A, Roeser J, Langenhahn T, Schwarze M, Schomäcker R, et al. Diacetylene
22 Functionalized Covalent Organic Framework (COF) for Photocatalytic Hydrogen Generation. *J Am*
23 *Chem Soc* 2018;140:1423–7. <https://doi.org/10.1021/jacs.7b11255>.
- 24 [75] Kumar P, Boukherroub R, Shankar K. Sunlight-driven water-splitting using two-dimensional
25 carbon based semiconductors. *J Mater Chem A* 2018;6:12876–931.
26 <https://doi.org/10.1039/c8ta02061b>.
- 27 [76] Dai C, Pan Y, Liu B. Conjugated Polymer Nanomaterials for Solar Water Splitting. *Adv Energy*
28 *Mater* 2020;10:2002474. <https://doi.org/10.1002/aenm.202002474>.
- 29 [77] Zhu T, Wu H Bin, Wang Y, Xu R, Lou XW. Formation of 1D hierarchical structures composed of
30 Ni3S2 nanosheets on CNTs backbone for supercapacitors and photocatalytic H2 production. *Adv*
31 *Energy Mater* 2012;2:1497–502. <https://doi.org/10.1002/aenm.201200269>.
- 32 [78] Chava RK, Do JY, Kang M. Smart Hybridization of Au Coupled CdS Nanorods with Few Layered
33 MoS2 Nanosheets for High Performance Photocatalytic Hydrogen Evolution Reaction. *ACS*
34 *Sustain Chem Eng* 2018;6:6445–57. <https://doi.org/10.1021/acssuschemeng.8b00249>.
- 35 [79] Zhang M, Sun R, Li Y, Shi Q, Xie L, Chen J, et al. High H2 Evolution from Quantum Cu(II) Nanodot-
36 Doped Two-Dimensional Ultrathin TiO2 Nanosheets with Dominant Exposed {001} Facets for
37 Reforming Glycerol with Multiple Electron Transport Pathways. *J Phys Chem C* 2016;120:10746–
38 56. <https://doi.org/10.1021/acs.jpcc.6b01030>.

- 1 [80] Xu Q, Zhu B, Jiang C, Cheng B, Yu J. Constructing 2D/2D Fe₂O₃/g-C₃N₄ Direct Z-Scheme
2 Photocatalysts with Enhanced H₂ Generation Performance. *Sol RRL* 2018;2:1800006.
3 <https://doi.org/10.1002/solr.201800006>.
- 4 [81] Pavliuk M V., Fernandes AB, Abdellah M, Fernandes DLA, Machado CO, Rocha I, et al. Nano-
5 hybrid plasmonic photocatalyst for hydrogen production at 20% efficiency. *Sci Rep* 2017;7:1–9.
6 <https://doi.org/10.1038/s41598-017-09261-7>.
- 7 [82] Khon E, Lambright K, Khnayzer RS, Moroz P, Perera D, Butaeva E, et al. Improving the catalytic
8 activity of semiconductor nanocrystals through selective domain etching. *Nano Lett*
9 2013;13:2016–23. <https://doi.org/10.1021/nl400715n>.
- 10 [83] Kalisman P, Nakibli Y, Amirav L. Perfect Photon-to-Hydrogen Conversion Efficiency. *Nano Lett*
11 2016;16:1776–81. <https://doi.org/10.1021/acs.nanolett.5b04813>.
- 12 [84] Moroz P, Boddy A, Zamkov M. Challenges and prospects of photocatalytic applications utilizing
13 semiconductor nanocrystals. *Front Chem* 2018;6. <https://doi.org/10.3389/fchem.2018.00353>.
- 14 [85] Lu J, Zhang K, Liu XF, Zhang H, Sum TC, Neto AHC, et al. Order-disorder transition in a two-
15 dimensional boron-carbon-nitride alloy. *Nat Commun* 2013;4:1–7.
16 <https://doi.org/10.1038/ncomms3681>.
- 17 [86] Pati PB, Damas G, Tian L, Fernandes DLA, Zhang L, Pehlivan IB, et al. An experimental and
18 theoretical study of an efficient polymer nano-photocatalyst for hydrogen evolution. *Energy*
19 *Environ Sci* 2017;10:1372–6. <https://doi.org/10.1039/c7ee00751e>.
- 20 [87] Ye S, Wang R, Wu MZ, Yuan YP. A review on g-C₃N₄ for photocatalytic water splitting and CO₂
21 reduction. *Appl Surf Sci* 2015;358:15–27. <https://doi.org/10.1016/j.apsusc.2015.08.173>.
- 22 [88] Kondarides DI, Daskalaki VM, Patsoura A, Verykios XE. Hydrogen production by photo-induced
23 reforming of biomass components and derivatives at ambient conditions. *Catal Letters*
24 2008;122:26–32. <https://doi.org/10.1007/s10562-007-9330-3>.
- 25 [89] Anthony Raja M, Preethi V. Photocatalytic hydrogen production using bench-scale trapezoidal
26 photocatalytic reactor. *Int J Hydrogen Energy* 2020;45:7574–83.
27 <https://doi.org/10.1016/j.ijhydene.2019.08.204>.
- 28 [90] El-Maghrabi HH, Ali HR, Younis SA. Construction of a new ternary α -MoO₃-WO₃/CdS solar
29 nanophotocatalyst towards clean water and hydrogen production from artificial wastewater
30 using optimal design methodology. *RSC Adv* 2017;7:4409–21.
31 <https://doi.org/10.1039/c6ra25146c>.
- 32 [91] Kaur K, Singh CV. Amorphous TiO₂ as a photocatalyst for hydrogen production: A DFT study of
33 structural and electronic properties. *Energy Procedia* 2012;29:291–9.
34 <https://doi.org/10.1016/j.egypro.2012.09.035>.
- 35 [92] Hanaor DAH, Assadi MHN, Li S, Yu A, Sorrell CC. Ab initio study of phase stability in doped TiO₂.
36 *Comput Mech* 2012;50:185–94. <https://doi.org/10.1007/s00466-012-0728-4>.
- 37 [93] Das B, Choudhury B, Gomathi A, Manna AK, Pati SK, Rao CNR. Interaction of inorganic
38 nanoparticles with graphene. *ChemPhysChem* 2011;12:937–43.

- 1 <https://doi.org/10.1002/cphc.201001090>.
- 2 [94] Kanda S, Akita T, Fujishima M, Tada H. Facile synthesis and catalytic activity of MoS₂/TiO₂ by a
3 photodeposition-based technique and its oxidized derivative MoO₃/TiO₂ with a unique
4 photochromism. *J Colloid Interface Sci* 2011;354:607–10.
5 <https://doi.org/10.1016/j.jcis.2010.11.007>.
- 6 [95] Srivastava N, Srivastava M, Mishra PK, Kausar MA, Saeed M, Gupta VK, et al. Advances in
7 nanomaterials induced biohydrogen production using waste biomass. *Bioresour Technol*
8 2020;307:123094. <https://doi.org/10.1016/j.biortech.2020.123094>.
- 9 [96] Lin R, Cheng J, Ding L, Song W, Liu M, Zhou J, et al. Enhanced dark hydrogen fermentation by
10 addition of ferric oxide nanoparticles using *Enterobacter aerogenes*. *Bioresour Technol*
11 2016;207:213–9. <https://doi.org/10.1016/j.biortech.2016.02.009>.
- 12 [97] Taherdanak M, Zilouei H, Karimi K. Investigating the effects of iron and nickel nanoparticles on
13 dark hydrogen fermentation from starch using central composite design. *Int J Hydrogen Energy*
14 2015;40:12956–63. <https://doi.org/10.1016/j.ijhydene.2015.08.004>.
- 15 [98] Ladole MR, Mevada JS, Pandit AB. Ultrasonic hyperactivation of cellulase immobilized on
16 magnetic nanoparticles. *Bioresour Technol* 2017;239:117–26.
17 <https://doi.org/10.1016/j.biortech.2017.04.096>.
- 18 [99] Srivastava N, Srivastava M, Manikanta A, Singh P, Ramteke PW, Mishra PK. Nanomaterials for
19 biofuel production using lignocellulosic waste. *Environ Chem Lett* 2017;15:179–84.
20 <https://doi.org/10.1007/s10311-017-0622-6>.
- 21 [100] Sambusiti C, Bellucci M, Zabaniotou A, Beneduce L, Monlau F. Algae as promising feedstocks for
22 fermentative biohydrogen production according to a biorefinery approach: A comprehensive
23 review. *Renew Sustain Energy Rev* 2015;44:20–36. <https://doi.org/10.1016/j.rser.2014.12.013>.
- 24 [101] Engliman NS, Abdul PM, Wu SY, Jahim JM. Influence of iron (II) oxide nanoparticle on
25 biohydrogen production in thermophilic mixed fermentation. *Int J Hydrogen Energy*
26 2017;42:27482–93. <https://doi.org/10.1016/j.ijhydene.2017.05.224>.
- 27 [102] Wang J, Wan W. Influence of Ni²⁺ concentration on biohydrogen production. *Bioresour Technol*
28 2008;99:8864–8. <https://doi.org/10.1016/j.biortech.2008.04.052>.
- 29 [103] Han H, Cui M, Wei L, Yang H, Shen J. Enhancement effect of hematite nanoparticles on
30 fermentative hydrogen production. *Bioresour Technol* 2011;102:7903–9.
31 <https://doi.org/10.1016/j.biortech.2011.05.089>.
- 32 [104] Liu B, Jin Y, Wang Z, Xing D, Ma C, Ding J, et al. Enhanced photo-fermentative hydrogen
33 production of *Rhodospseudomonas* sp. nov. strain A7 by the addition of TiO₂, ZnO and SiC
34 nanoparticles. *Int J Hydrogen Energy* 2017;42:18279–87.
35 <https://doi.org/10.1016/j.ijhydene.2017.04.147>.
- 36 [105] Okolie JA, Mukherjee A, Nanda S, Dalai AK, Kozinski JA. Catalytic Supercritical Water Gasification
37 of Soybean Straw: Effects of Catalyst Supports and Promoters. *Ind Eng Chem Res* 2021;60:5770–
38 82. <https://doi.org/10.1021/acs.iecr.0c06177>.

- 1 [106] Norouzi O, Safari F, Jafarian S, Tavasoli A, Karimi A. Hydrothermal gasification performance of
2 Enteromorpha intestinalis as an algal biomass for hydrogen-rich gas production using Ru
3 promoted Fe–Ni/γ-Al₂O₃ nanocatalysts. *Energy Convers Manag* 2017;141:63–71.
4 <https://doi.org/10.1016/j.enconman.2016.04.083>.
- 5 [107] Velusamy K, Devanand J, Senthil Kumar P, Soundarajan K, Sivasubramanian V, Sindhu J, et al. A
6 review on nano-catalysts and biochar-based catalysts for biofuel production. *Fuel*
7 2021;306:121632. <https://doi.org/10.1016/j.fuel.2021.121632>.
- 8 [108] Barati M, Babatabar M, Tavasoli A, Dalai AK, Das U. Hydrogen production via supercritical water
9 gasification of bagasse using unpromoted and zinc promoted Ru/γ-Al₂O₃ nanocatalysts. *Fuel*
10 *Process Technol* 2014;123:140–8. <https://doi.org/10.1016/j.fuproc.2014.02.005>.
- 11 [109] Rashidi M, Tavasoli A. Hydrogen rich gas production via supercritical water gasification of
12 sugarcane bagasse using unpromoted and copper promoted Ni/CNT nanocatalysts. *J Supercrit*
13 *Fluids* 2015;98:111–8. <https://doi.org/10.1016/j.supflu.2015.01.008>.
- 14 [110] Cao C, Xie Y, Mao L, Wei W, Shi J, Jin H. Hydrogen production from supercritical water gasification
15 of soda black liquor with various metal oxides. *Renew Energy* 2020;157:24–32.
16 <https://doi.org/10.1016/j.renene.2020.04.143>.
- 17 [111] Cao C, Zhang Y, Cao W, Jin H, Guo L, Huo Z. Transition Metal Oxides as Catalysts for Hydrogen
18 Production from Supercritical Water Gasification of Glucose. *Catal Letters* 2017;147:828–36.
19 <https://doi.org/10.1007/s10562-017-2002-z>.
- 20 [112] Nanda S, Reddy SN, Dalai AK, Kozinski JA. Subcritical and supercritical water gasification of
21 lignocellulosic biomass impregnated with nickel nanocatalyst for hydrogen production. *Int J*
22 *Hydrogen Energy* 2016;41:4907–21. <https://doi.org/10.1016/j.ijhydene.2015.10.060>.
- 23 [113] Kumar A, Reddy SN. Subcritical and supercritical water in-situ gasification of metal (Ni/Ru/Fe)
24 impregnated banana pseudo-stem for hydrogen rich fuel gas mixture. *Int J Hydrogen Energy*
25 2020;45:18348–62. <https://doi.org/10.1016/j.ijhydene.2019.08.009>.
- 26 [114] Moradi R, Groth KM. Hydrogen storage and delivery: Review of the state of the art technologies
27 and risk and reliability analysis. *Int J Hydrogen Energy* 2019;44:12254–69.
28 <https://doi.org/10.1016/j.ijhydene.2019.03.041>.
- 29 [115] Rusman NAA, Dahari M. A review on the current progress of metal hydrides material for solid-
30 state hydrogen storage applications. *Int J Hydrogen Energy* 2016;41:12108–26.
31 <https://doi.org/10.1016/j.ijhydene.2016.05.244>.
- 32 [116] Zhevago NK, Chabak AF, Denisov EI, Glebov VI, Korobtsev S V. Storage of cryo-compressed
33 hydrogen in flexible glass capillaries. *Int J Hydrogen Energy* 2013;38:6694–703.
34 <https://doi.org/10.1016/j.ijhydene.2013.03.107>.
- 35 [117] Keçebaş A, Kayfeci M. Hydrogen properties. *Sol. Hydrog. Prod. Process. Syst. Technol.*, Elsevier;
36 2019, p. 3–29. <https://doi.org/10.1016/B978-0-12-814853-2.00001-1>.
- 37 [118] Durbin DJ, Malardier-Jugroot C. Review of hydrogen storage techniques for on board vehicle
38 applications. *Int J Hydrogen Energy* 2013;38:14595–617.
39 <https://doi.org/10.1016/j.ijhydene.2013.07.058>.

- 1 [119] Peschel A. Industrial Perspective on Hydrogen Purification, Compression, Storage, and
2 Distribution. *Fuel Cells* 2020;20:385–93. <https://doi.org/10.1002/fuce.201900235>.
- 3 [120] Berstad DO, Stang JH, Neksa P. Large-scale hydrogen liquefier utilising mixed-refrigerant pre-
4 cooling. *Int J Hydrogen Energy* 2010;35:4512–23.
5 <https://doi.org/10.1016/j.ijhydene.2010.02.001>.
- 6 [121] Tarhan C, Çil MA. A study on hydrogen, the clean energy of the future: Hydrogen storage
7 methods. *J Energy Storage* 2021;40:102676. <https://doi.org/10.1016/j.est.2021.102676>.
- 8 [122] Elberry AM, Thakur J, Santasalo-Aarnio A, Larimi M. Large-scale compressed hydrogen storage as
9 part of renewable electricity storage systems. *Int J Hydrogen Energy* 2021;46:15671–90.
10 <https://doi.org/10.1016/j.ijhydene.2021.02.080>.
- 11 [123] Ozaki M, Tomura S, Ohmura R, Mori YH. Comparative study of large-scale hydrogen storage
12 technologies: Is hydrate-based storage at advantage over existing technologies? *Int J Hydrogen*
13 *Energy* 2014;39:3327–41. <https://doi.org/10.1016/j.ijhydene.2013.12.080>.
- 14 [124] Bossel U, Eliasson B. Energy and the Hydrogen Economy. ABB Switz Ltd 2009:1–35.
15 https://afdc.energy.gov/files/pdfs/hyd_economy_bossel_eliasson.pdf; (accessed December 15,
16 2021).
- 17 [125] Niaz S, Manzoor T, Energy AP-R and S, 2015 U. Hydrogen storage: Materials, methods and
18 perspectives. Elsevier 2015.
- 19 [126] Bracha M, Lorenz G, Patzelt A, Wanner M. Large-scale hydrogen liquefaction in Germany. *Int J*
20 *Hydrogen Energy* 1994;19:53–9. [https://doi.org/10.1016/0360-3199\(94\)90177-5](https://doi.org/10.1016/0360-3199(94)90177-5).
- 21 [127] Kumar A, Raju NN, Muthukumar P, Selvan PV. Experimental studies on industrial scale metal
22 hydride based hydrogen storage system with embedded cooling tubes. *Int J Hydrogen Energy*
23 2019;44:13549–60. <https://doi.org/10.1016/j.ijhydene.2019.03.180>.
- 24 [128] Chauhan PK, Parameshwaran R, Kannan P, Madhavaram R, Sujith R. Hydrogen storage in porous
25 polymer derived SiliconOxycarbide ceramics: Outcomes and perspectives. *Ceram Int*
26 2021;47:2591–9. <https://doi.org/10.1016/J.CERAMINT.2020.09.105>.
- 27 [129] Souahlia A, Dhaou H, Mellouli S, Askri F, Jemni A, Ben Nasrallah S. Experimental study of metal
28 hydride-based hydrogen storage tank at constant supply pressure. *Int J Hydrogen Energy*
29 2014;39:7365–72. <https://doi.org/10.1016/j.ijhydene.2014.02.121>.
- 30 [130] Cheng HM, Yang QH, Liu C. Hydrogen storage in carbon nanotubes. *Carbon N Y* 2001;39:1447–54.
31 [https://doi.org/10.1016/S0008-6223\(00\)00306-7](https://doi.org/10.1016/S0008-6223(00)00306-7).
- 32 [131] Li Y, Liu H. Grand canonical Monte Carlo simulation on the hydrogen storage behaviors of the
33 cup-stacked carbon nanotubes at room temperature. *Int J Hydrogen Energy* 2021;46:6623–31.
34 <https://doi.org/10.1016/j.ijhydene.2020.11.139>.
- 35 [132] Rather S ullah. Preparation, characterization and hydrogen storage studies of carbon nanotubes
36 and their composites: A review. *Int J Hydrogen Energy* 2020;45:4653–72.
37 <https://doi.org/10.1016/j.ijhydene.2019.12.055>.

- 1 [133] He H, Pham-Huy LA, Dramou P, Xiao D, Zuo P, Pham-Huy C. Carbon nanotubes: Applications in
2 pharmacy and medicine. *Biomed Res Int* 2013;2013. <https://doi.org/10.1155/2013/578290>.
- 3 [134] Patel DK, Kim H, Dutta SD, Ganguly K, Lim K. Carbon Nanotubes-Based Nanomaterials and Their
4 Agricultral and Biotechnological Applications. *Materials (Basel)* 2020;1–28.
- 5 [135] Mohan M, Sharma VK, Kumar EA, Gayathri V. Hydrogen storage in carbon materials-Areview.
6 *Energy Storage* 2010;1–26. <https://doi.org/10.1002/est2.35>.
- 7 [136] Panella B, Hirscher M, Roth S. Hydrogen adsorption in different carbon nanostructures. *Carbon N*
8 *Y* 2005;43:2209–14. <https://doi.org/10.1016/j.carbon.2005.03.037>.
- 9 [137] Park C, Keane MA. Controlled Growth of Highly Ordered Carbon Nanofibers from Y Zeolite
10 Supported Nickel Catalysts. *Langmuir* 2001;17:8386–96.
- 11 [138] Li, X., Zhu, H., Ci, L., Xu, C., Mao, Z., Wei, B., et al. Hydrogen uptake by graphitized multi-walled
12 carbon nanotubes under moderate pressure and at room temperature. *Carbon N Y* n.d.
- 13 [139] Tozzini V, Pellegrini V. Prospects for hydrogen storage in graphene. *Phys Chem Chem Phys*
14 2013;15:80–9. <https://doi.org/10.1039/c2cp42538f>.
- 15 [140] Dillon AC, Heben MJ. Hydrogen storage using carbon adsorbents : past , present and future. *Appl*
16 *Phys A* 2001;72:133–42.
- 17 [141] Dillon AC, Jones KM, Bekkedahl TA, Kiang CH, Bethune DS, Heben MJ. Storage of hydrogen in
18 single-walled carbon nanotubes. *Nature* 1997;386:377–9.
- 19 [142] Huang CW, Wu HC, Li YY. Hydrogen storage in platelet graphite nanofibers. *Sep Purif Technol*
20 2007;58:219–23. <https://doi.org/10.1016/j.seppur.2007.07.032>.
- 21 [143] Dillon AC., Jones KM., Bekkedahl TA., Klangt CH, Bethunet DS, Heben MJ. Storafe of hydrogen in
22 single-walled carbon nanotubes. *Lett to Nat* 1997;668:1995–7.
- 23 [144] Yu X, Tang Z, Sun D, Ouyang L, Zhu M. Recent advances and remaining challenges of
24 nanostructured materials for hydrogen storage applications. *Prog Mater Sci* 2017;88:1–48.
25 <https://doi.org/10.1016/j.pmatsci.2017.03.001>.
- 26 [145] Ioannatos GE, Verykios XE. H2 storage on single- and multi-walled carbon nanotubes. *Int J*
27 *Hydrogen Energy* 2010;35:622–8. <https://doi.org/10.1016/j.ijhydene.2009.11.029>.
- 28 [146] Shalabi AS, Abdel Halim WS, Abdel Aal S, Soliman KA. Tuning hydrogen storage of carbon
29 nanotubes by mechanical bending: Theoretical study. *Mol Simul* 2016;42:709–14.
30 <https://doi.org/10.1080/08927022.2015.1085122>.
- 31 [147] Srinivasan S, Demirocak DE, Kaushik A, Sharma M, Chaudhary GR, Hickman N, et al. Reversible
32 hydrogen storage using nanocomposites. *Appl Sci* 2020;10.
33 <https://doi.org/10.3390/app10134618>.
- 34 [148] Salehabadi A, Umar MF, Ahmad A, Ahmad MI, Ismail N, Rafatullah M. Carbon-based
35 nanocomposites in solid-state hydrogen storage technology: An overview. *Int J Energy Res*
36 2020;44. <https://doi.org/10.1002/er.5674>.

- 1 [149] Yan Y, Au YS, Rentsch D, Remhof A, De Jongh PE, Züttel A. Reversible hydrogen storage in
2 Mg(BH₄)₂/carbon nanocomposites. *J Mater Chem A* 2013;1.
3 <https://doi.org/10.1039/c3ta12222k>.
- 4 [150] Ward PA, Teprovich JA, Peters B, Wheeler J, Compton RN, Zidan R. Reversible hydrogen storage
5 in a LiBH₄-C₆₀ nanocomposite. *J Phys Chem C* 2013;117. <https://doi.org/10.1021/jp4079103>.
- 6 [151] Gross AF, Vajo JJ, Van Atta SL, Olson GL. Enhanced hydrogen storage kinetics of LiBH₄ in
7 nanoporous carbon scaffolds. *J Phys Chem C* 2008;112. <https://doi.org/10.1021/jp711066t>.
- 8 [152] Li L, Yao X, Sun C, Du A, Cheng L, Zhu Z, et al. Lithium-catalyzed dehydrogenation of ammonia
9 borane within mesoporous carbon framework for chemical hydrogen storage. *Adv Funct Mater*
10 2009;19. <https://doi.org/10.1002/adfm.200801111>.
- 11 [153] Zhao-Karger Z, Witter R, Bardají EG, Wang D, Cossement D, Fichtner M. Altered reaction
12 pathways of eutectic LiBH₄-Mg(BH₄)₂ by nanoconfinement. *J Mater Chem A* 2013;1.
13 <https://doi.org/10.1039/c2ta00542e>.
- 14 [154] Gao J, Ngene P, Herrich M, Xia W, Gutfleisch O, Muhler M, et al. Interface effects in NaAlH₄-
15 carbon nanocomposites for hydrogen storage. *Int J Hydrogen Energy* 2014;39:10175–83.
16 <https://doi.org/10.1016/j.ijhydene.2014.03.188>.
- 17 [155] Feaver A, Sepehri S, Shamberger P, Stowe A, Autrey T, Cao G. Coherent carbon cryogel-ammonia
18 borane nanocomposites for H₂ storage. *J Phys Chem B* 2007;111.
19 <https://doi.org/10.1021/jp072448t>.
- 20 [156] Sepehri S, Garcia BB, Cao G. Tuning dehydrogenation temperature of carbon-ammonia borane
21 nanocomposites. *J Mater Chem* 2008;18. <https://doi.org/10.1039/b808511k>.
- 22 [157] Figueroa-Torres MZ, Domínguez-Ríos C, Cabañas-Moreno JG, Vega-Becerra O, Aguilar-Elguézabal
23 A. The synthesis of Ni-activated carbon nanocomposites via electroless deposition without a
24 surface pretreatment as potential hydrogen storage materials. *Int J Hydrogen Energy* 2012;37.
25 <https://doi.org/10.1016/j.ijhydene.2012.04.097>.
- 26 [158] Bravo Diaz L, Hanlon JM, Bielewski M, Milewska A, Gregory DH. Ammonia Borane Based
27 Nanocomposites as Solid-State Hydrogen Stores for Portable Power Applications. *Energy Technol*
28 2018;6. <https://doi.org/10.1002/ente.201700651>.
- 29 [159] Zhu C, Chen M, Hu M, He D, Liu Y, Liu T. Hydrogen storage properties of Mg–Nb@C
30 nanocomposite: Effects of Nb nanocatalyst and carbon nanoconfinement. *Int J Hydrogen Energy*
31 2021;46. <https://doi.org/10.1016/j.ijhydene.2020.12.099>.
- 32 [160] Liu Y, Zou J, Zeng X, Wu X, Tian H, Ding W, et al. Study on hydrogen storage properties of Mg
33 nanoparticles confined in carbon aerogels. *Int. J. Hydrogen Energy*, vol. 38, 2013.
34 <https://doi.org/10.1016/j.ijhydene.2013.02.012>.
- 35 [161] Cahen S, Eymery JB, Janot R, Tarascon JM. Improvement of the LiBH₄ hydrogen desorption by
36 inclusion into mesoporous carbons. *J Power Sources* 2009;189.
37 <https://doi.org/10.1016/j.jpowsour.2009.01.002>.
- 38 [162] Mukherjee A, Okolie JA, Abdelrasoul A, Niu C, Dalai AK. Review of post-combustion carbon

- 1 dioxide capture technologies using activated carbon. *J Environ Sci* 2019;83:46–63.
2 <https://doi.org/10.1016/J.JES.2019.03.014>.
- 3 [163] Strobel R, Garche J, Moseley PT, Wolf G, Institut F. Hydrogen storage by carbon materials. *J*
4 *Power Sources* 2006;159:781–801. <https://doi.org/10.1016/j.jpowsour.2006.03.047>.
- 5 [164] Rajalakshmi N, Ramesh T. Activated Carbons-Promising Materials- Hydrogen Perspective. *Agric*
6 *Res Technol Open Access J* 2017;10:1–3. <https://doi.org/10.19080/ARTOAJ.2017.10.555776>.
- 7 [165] Czarna-Juszkiewicz D, Cader J, Wdowin M. From coal ashes to solid sorbents for hydrogen
8 storage. *J Clean Prod* 2020;270:122355. <https://doi.org/10.1016/j.jclepro.2020.122355>.
- 9 [166] Kapasiti P, Hidrogen P, Aktifan K. Hydrogen Adsorption Capacity Reduction of Activated Carbon
10 Produced from Indonesia Low Rank Coal by Pelletizing. *Sains Malays* 2015;44:747–52.
- 11 [167] Zhao W, Luo L, Chen T, Li Z, Zhang Z, Fan M. Activated carbons from oil palm shell for hydrogen
12 storage. *IOP Conf. Ser. Mater. Sci. Eng.*, vol. 368, 2018, p. 368. [https://doi.org/10.1088/1757-](https://doi.org/10.1088/1757-899X/368/1/012031)
13 [899X/368/1/012031](https://doi.org/10.1088/1757-899X/368/1/012031).
- 14 [168] Akasaka H, Takahata T, Toda I, Ono H, Ohshio S. Hydrogen storage ability of porous carbon
15 material fabricated from coffee bean wastes. *Int J Hydrogen Energy* 2010;36:580–5.
16 <https://doi.org/10.1016/j.ijhydene.2010.09.102>.
- 17 [169] Fierro V, Szczurek A, Zlotea C, Mareche JF, Izquierdo MT, Albiniak A, et al. Experimental evidence
18 of an upper limit for hydrogen storage at 77 K on activated carbons. *Carbon N Y* 2010;48:1902–
19 11. <https://doi.org/10.1016/j.carbon.2010.01.052>.
- 20 [170] Alfadlil BR, Knowles GP, Parsa MR, Subagyono RRDJN, Daniel, Chaffee AL. Carbon monolith from
21 Victorian brown coal for hydrogen storage. *J Phys Conf Ser* 2019;1277:1–7.
22 <https://doi.org/10.1088/1742-6596/1277/1/012024>.
- 23 [171] Xu W, Takahashi K, Matsuo Y, Hattori Y, Kumagai M, Ishiyama S, et al. Investigation of hydrogen
24 storage capacity of various carbon materials. *Int J Hydrogen Energy* 2007;32:2504–12.
25 <https://doi.org/10.1016/j.ijhydene.2006.11.012>.
- 26 [172] Izquierdo MT, Celzard A. Impact of synthesis conditions of KOH activated carbons on their
27 hydrogen storage capacities 2012;7:3–9. <https://doi.org/10.1016/j.ijhydene.2012.06.110>.
- 28 [173] Zhao W, Fierro V, Zlotea C, Izquierdo MT, Chevalier-César C, Latroche M, et al. Activated carbons
29 doped with Pd nanoparticles for hydrogen storage. *Int J Hydrogen Energy* 2012;37:5072–80.
30 <https://doi.org/10.1016/j.ijhydene.2011.12.058>.
- 31 [174] Orimo SI, Nakamori Y, Eliseo JR, Züttel A, Jensen CM. Complex hydrides for hydrogen storage.
32 *Chem Rev* 2007;107:4111–32. <https://doi.org/10.1021/cr0501846>.
- 33 [175] He T, Cao H, Chen P. Complex Hydrides for Energy Storage, Conversion, and Utilization. *Adv*
34 *Mater* 2019;31:1902757. <https://doi.org/10.1002/adma.201902757>.
- 35 [176] Møller KT, Sheppard D, Ravnsbæk DB, Buckley CE, Akiba E, Li HW, et al. Complex metal hydrides
36 for hydrogen, thermal and electrochemical energy storage. *Energies* 2017;10:1645.
37 <https://doi.org/10.3390/en10101645>.

- 1 [177] Andersson J, Grönkvist S. Large-scale storage of hydrogen. *Int J Hydrogen Energy* 2019;44:11901–
2 19. <https://doi.org/10.1016/j.ijhydene.2019.03.063>.
- 3 [178] Ley MB, Jepsen LH, Lee YS, Cho YW, Bellosta Von Colbe JM, Dornheim M, et al. Complex hydrides
4 for hydrogen storage - New perspectives. *Mater Today* 2014;17:122–8.
5 <https://doi.org/10.1016/j.mattod.2014.02.013>.
- 6 [179] Gupta A, Baron G V., Perreault P, Lenaerts S, Ciocarlan RG, Cool P, et al. Hydrogen Clathrates:
7 Next Generation Hydrogen Storage Materials. *Energy Storage Mater* 2021;41:69–107.
8 <https://doi.org/10.1016/j.ensm.2021.05.044>.
- 9 [180] Luo Y, Wang Q, Li J, Xu F, Sun L, Zou Y, et al. Enhanced hydrogen storage/sensing of metal
10 hydrides by nanomodification. *Mater Today Nano* 2020;9:100071.
11 <https://doi.org/10.1016/j.mtnano.2019.100071>.
- 12 [181] Zhang X, Ren Z, Zhang X, Gao M, Pan H, Liu Y. Triggering highly stable catalytic activity of metallic
13 titanium for hydrogen storage in NaAlH₄ by preparing ultrafine nanoparticles. *J Mater Chem A*
14 2019;7:4651–9. <https://doi.org/10.1039/c9ta00748b>.
- 15 [182] Santoru A, Pistidda C, Brighi M, Chierotti MR, Heere M, Karimi F, et al. Insights into the Rb-Mg-N-
16 H System: An Ordered Mixed Amide/Imide Phase and a Disordered Amide/Hydride Solid Solution.
17 *Inorg Chem* 2018;57:3197–205. <https://doi.org/10.1021/acs.inorgchem.7b03232>.
- 18 [183] Pohlmann C, Röntzsch L, Hu J, Weißgärber T, Kieback B, Fichtner M. Tailored heat transfer
19 characteristics of pelletized LiNH₂-MgH₂ and NaAlH₄ hydrogen storage materials. *J Power*
20 *Sources* 2012;205:173–9. <https://doi.org/10.1016/j.jpowsour.2012.01.064>.
- 21 [184] Milanese C, Garroni S, Gennari F, Marini A, Klassen T, Dornheim M, et al. Solid state hydrogen
22 storage in alanates and alanate-based compounds: A review. *Metals (Basel)* 2018;8:567.
23 <https://doi.org/10.3390/met8080567>.
- 24 [185] Fan X, Xiao X, Chen L, Zhang L, Shao J, Li S, et al. Significantly improved hydrogen storage
25 properties of NaAlH₄ catalyzed by Ce-based nanoparticles. *J Mater Chem A* 2013;1:9752–9.
26 <https://doi.org/10.1039/c3ta11860f>.
- 27 [186] Baldé CP, Hereijgers BPC, Bitter JH, De Jong KP. Sodium alanate nanoparticles - Linking size to
28 hydrogen storage properties. *J Am Chem Soc* 2008;130:6761–5.
29 <https://doi.org/10.1021/ja710667v>.
- 30 [187] Zheng S, Fang F, Zhou G, Chen G, Ouyang L, Zhu M, et al. Hydrogen storage properties of space-
31 confined NaAlH₄ nanoparticles in ordered mesoporous silica. *Chem Mater* 2008;20:3954–8.
32 <https://doi.org/10.1021/cm8002063>.
- 33 [188] Liu Y, Zhang X, Wang K, Yang Y, Gao M, Pan H. Achieving ambient temperature hydrogen storage
34 in ultrafine nanocrystalline TiO₂@C-doped NaAlH₄. *J Mater Chem A* 2016;4:1087–95.
35 <https://doi.org/10.1039/c5ta09400c>.
- 36 [189] Zhang X, Ren Z, Lu Y, Yao J, Gao M, Liu Y, et al. Facile Synthesis and Superior Catalytic Activity of
37 Nano-TiN@N-C for Hydrogen Storage in NaAlH₄. *ACS Appl Mater Interfaces* 2018;10:15767–77.
38 <https://doi.org/10.1021/acsami.8b04011>.

- 1 [190] Li L, Qiu F, Wang Y, Liu G, Xu Y, An C, et al. TiN catalyst for the reversible hydrogen storage
2 performance of sodium alanate system. *J Mater Chem* 2012;22:13782–7.
3 <https://doi.org/10.1039/c2jm31388j>.
- 4 [191] Arora E, Saini S, Basera P, Kumar M, Singh A, Bhattacharya S. Elucidating the Role of Temperature
5 and Pressure to the Thermodynamic Stability of Charged Defects in Complex Metal-Hydrides: A
6 Case Study of NaAlH₄. *J Phys Chem C* 2019;123:62–9. <https://doi.org/10.1021/acs.jpcc.8b08687>.
- 7 [192] Kang SY, Heo TW, Allendorf MD, Wood BC. Morphology-Dependent Stability of Complex Metal
8 Hydrides and Their Intermediates Using First-Principles Calculations. *ChemPhysChem*
9 2019;20:1340–7. <https://doi.org/10.1002/cphc.201801132>.
- 10 [193] Züttel A, Borgschulte A, Orimo SI. Tetrahydroborates as new hydrogen storage materials. *Scr*
11 *Mater* 2007;56:823–8. <https://doi.org/10.1016/j.scriptamat.2007.01.010>.
- 12 [194] Lai Q, Aguey-Zinsou KF. Destabilisation of Ca(BH₄)₂ and Mg(BH₄)₂: Via confinement in
13 nanoporous Cu₂S hollow spheres. *Sustain Energy Fuels* 2017;1:1308–19.
14 <https://doi.org/10.1039/c7se00121e>.
- 15 [195] Huang Z, Wang Y, Wang D, Yang F, Wu Z, Zhang Z. Influence of transition metals Fe, Co, Ni, Cu
16 and Ti on the dehydrogenation characteristics of LiBH₄: A first-principles investigation. *Comput*
17 *Theor Chem* 2018;1133:33–9. <https://doi.org/10.1016/j.comptc.2018.04.017>.
- 18 [196] Chen P, Xiong Z, Luo J, Lin J, Lee Tan K. Interaction of hydrogen with metal nitrides and imides.
19 *Nature* 2002;420:302–4. <https://doi.org/10.1038/nature01210>.
- 20 [197] Wood BC, Heo TW, Kang S, Wan LF, Li S. Beyond Idealized Models of Nanoscale Metal Hydrides
21 for Hydrogen Storage. *Ind Eng Chem Res* 2020;59:5786–96.
22 <https://doi.org/10.1021/acs.iecr.9b06617>.
- 23 [198] Cao H, Pistidda C, Richter TMM, Santoru A, Milanese C, Garroni S, et al. In situ x-ray diffraction
24 studies on the de/rehydrogenation processes of the K₂[Zn(NH₂)₄]-8LiH system. *J Phys Chem C*
25 2017;121:1546–51. <https://doi.org/10.1021/acs.jpcc.6b12095>.
- 26 [199] Shaw LL, Ren R, Markmaitree T, Osborn W. Effects of mechanical activation on dehydrogenation
27 of the lithium amide and lithium hydride system. *J Alloys Compd* 2008;448:263–71.
28 <https://doi.org/10.1016/j.jallcom.2006.10.029>.
- 29 [200] Zhou HCJ, Kitagawa S. Metal-Organic Frameworks (MOFs). *Chem Soc Rev* 2014;43:5415–8.
30 <https://doi.org/10.1039/c4cs90059f>.
- 31 [201] Janiak C. Engineering coordination polymers towards applications. *J Chem Soc Dalt Trans*
32 2003;3:2781–804. <https://doi.org/10.1039/b305705b>.
- 33 [202] Zeleňák V, Saldan I. Factors affecting hydrogen adsorption in metal-organic frameworks: A short
34 review. *Nanomaterials* 2021;11:1638. <https://doi.org/10.3390/nano11071638>.
- 35 [203] Lin X, Jia J, Champness NR, Hubberstey P, Schröder M. Metal-organic framework materials for
36 hydrogen storage. *Solid-State Hydrog Storage Mater Chem* 2008:288–312.
37 <https://doi.org/10.1533/9781845694944.3.288>.

- 1 [204] Sule R, Mishra AK, Nkambule TT. Recent advancement in consolidation of MOFs as absorbents for
2 hydrogen storage. *Int J Energy Res* 2021;45:12481–99. <https://doi.org/10.1002/er.6608>.
- 3 [205] Ockwig NW, Delgado-Friedrichs O, O’Keeffe M, Yaghi OM. Reticular chemistry: Occurrence and
4 taxonomy of nets and grammar for the design of frameworks. *Acc Chem Res* 2005;38:176–82.
5 <https://doi.org/10.1021/ar020022l>.
- 6 [206] U.S Department of Energy. DOE Technical Targets for Onboard Hydrogen Storage for Light-Duty
7 Vehicles | Department of Energy. *EnergyGov* 2017:1–23.
8 [https://www.energy.gov/eere/fuelcells/doe-technical-targets-onboard-hydrogen-storage-light-](https://www.energy.gov/eere/fuelcells/doe-technical-targets-onboard-hydrogen-storage-light-duty-vehicles%0Ahttps://energy.gov/eere/fuelcells/doe-technical-targets-onboard-hydrogen-storage-light-duty-vehicles)
9 [duty-vehicles%0Ahttps://energy.gov/eere/fuelcells/doe-technical-targets-onboard-hydrogen-](https://www.energy.gov/eere/fuelcells/doe-technical-targets-onboard-hydrogen-storage-light-duty-vehicles)
10 [storage-light-duty-vehicles](https://www.energy.gov/eere/fuelcells/doe-technical-targets-onboard-hydrogen-storage-light-duty-vehicles) (accessed September 1, 2021).
- 11 [207] Ahmed A, Liu Y, Purewal J, Tran LD, Wong-Foy AG, Veenstra M, et al. Balancing gravimetric and
12 volumetric hydrogen density in MOFs. *Energy Environ Sci* 2017;10:2459–71.
13 <https://doi.org/10.1039/c7ee02477k>.
- 14 [208] Collins DJ, Zhou HC. Hydrogen storage in metal-organic frameworks. *J Mater Chem*
15 2007;17:3154–60. <https://doi.org/10.1039/b702858j>.
- 16 [209] Yaghi OM, O’Keeffe M, Ockwig NW, Chae HK, Eddaoudi M, Kim J. Reticular synthesis and the
17 design of new materials. *Nature* 2003;423:705–14. <https://doi.org/10.1038/nature01650>.
- 18 [210] Koh K, Wong-Foy AG, Matzger AJ. A porous coordination copolymer with over 5000 m²/g BET
19 surface area. *J Am Chem Soc* 2009;131:4184–5. <https://doi.org/10.1021/ja809985t>.
- 20 [211] Klein N, Senkovska I, Gedrich K, Stoeck U, Henschel A, Mueller U, et al. A mesoporous metal-
21 organic framework. *Angew Chemie - Int Ed* 2009;48:9954–7.
22 <https://doi.org/10.1002/anie.200904599>.
- 23 [212] Deng H, Doonan CJ, Furukawa H, Ferreira RB, Towne J, Knobler CB, et al. Multiple functional
24 groups of varying ratios in metal-organic frameworks. *Science (80-)* 2010;327:846–50.
25 <https://doi.org/10.1126/science.1181761>.
- 26 [213] Ma L, Jin A, Xie Z, Lin W. Freeze drying significantly increases permanent porosity and hydrogen
27 uptake in 4,4-connected metal-organic frameworks. *Angew Chemie - Int Ed* 2009;48:9905–8.
28 <https://doi.org/10.1002/anie.200904983>.
- 29 [214] Cooper AI, Rosseinsky MJ. Metal-organic frameworks: Improving pore performance. *Nat Chem*
30 2009;1:26–7. <https://doi.org/10.1038/nchem.157>.
- 31 [215] Xiang Z, Cao D, Shao X, Wang W, Zhang J, Wu W. Facile preparation of high-capacity hydrogen
32 storage metal-organic frameworks: A combination of microwave-assisted solvothermal synthesis
33 and supercritical activation. *Chem Eng Sci* 2010;65:3140–6.
34 <https://doi.org/10.1016/J.CES.2010.02.005>.
- 35 [216] Zhou W, Wu H, Yildirim T. Enhanced H₂ adsorption in isostructural metal-organic frameworks
36 with open metal sites: Strong dependence of the binding strength on metal ions. *J Am Chem Soc*
37 2008;130:15268–9. <https://doi.org/10.1021/ja807023q>.
- 38 [217] Bagheri M, Masoomi MY, Domínguez E, García H. High hydrogen release catalytic activity by

- 1 quasi-MOFs prepared via post-synthetic pore engineering . Sustain Energy Fuels 2021.
2 <https://doi.org/10.1039/d1se00661d>.
- 3 [218] Rowsell JLC, Millward AR, Park KS, Yaghi OM. Hydrogen Sorption in Functionalized Metal-Organic
4 Frameworks. *J Am Chem Soc* 2004;126:5666–7. <https://doi.org/10.1021/ja049408c>.
- 5 [219] Mavrandonakis A, Tylianakis E, Stubos AK, Froudakis GE. Why Li doping in MOFs enhances H₂
6 storage capacity? A multi-scale theoretical study. *J Phys Chem C* 2008;112:7290–4.
7 <https://doi.org/10.1021/jp7102098>.
- 8 [220] Cheng H, Chen L, Cooper AC, Sha X, Pez GP. Hydrogen spillover in the context of hydrogen
9 storage using solid-state materials. *Energy Environ Sci* 2008;1:338–54.
10 <https://doi.org/10.1039/b807618a>.
- 11 [221] Suresh K, Aulakh D, Purewal J, Siegel DJ, Veenstra M, Matzger AJ. Optimizing Hydrogen Storage in
12 MOFs through Engineering of Crystal Morphology and Control of Crystal Size. *J Am Chem Soc*
13 2021;143:10727–34. <https://doi.org/10.1021/jacs.1c04926>.
- 14 [222] Kolotilov S V., Pavlishchuk V V. Effect of structural and thermodynamic factors on the sorption of
15 hydrogen by metal-organic framework compounds. *Theor Exp Chem* 2009;45:75–97.
16 <https://doi.org/10.1007/s11237-009-9068-7>.
- 17 [223] Mao WL, Mao H. Hydrogen storage in molecular compounds. *Proc Natl Acad Sci* 2004;101:708–
18 10. <https://doi.org/10.1073/PNAS.0307449100>.
- 19 [224] Struzhkin V V., Militzer B, Mao WL, Mao HK, Hemley RJ. Hydrogen storage in molecular
20 clathrates. *Chem Rev* 2007;107:4133–51. <https://doi.org/10.1021/cr050183d>.
- 21 [225] Chattaraj PK, Bandaru S, Mondal S. Hydrogen storage in clathrate hydrates. *J Phys Chem A*
22 2011;115:187–93. <https://doi.org/10.1021/jp109515a>.
- 23 [226] Mao WL, Mao H kwang, Goncharov AF, Struzhkin V V., Guo Q, Hu J, et al. Hydrogen clusters in
24 clathrate hydrate. *Science (80-)* 2002;297:2247–9. <https://doi.org/10.1126/science.1075394>.
- 25 [227] Florusse LJ, Peters CJ, Schoonman J, Hester KC, Koh CA, Dec SF, et al. Stable low-pressure
26 hydrogen clusters stored in a binary clathrate hydrate. *Science (80-)* 2004;306:469–71.
27 <https://doi.org/10.1126/science.1102076>.
- 28 [228] Du JW, Liang DQ, Dai XX, Li DL, Li XJ. Hydrate phase equilibrium for the (hydrogen + tert-
29 butylamine + water) system. *J Chem Thermodyn* 2011;43:617–21.
30 <https://doi.org/10.1016/j.jct.2010.11.018>.
- 31 [229] Du J, Wang L, Liang D, Li D. Phase equilibria and dissociation enthalpies of hydrogen semi-
32 clathrate hydrate with tetrabutyl ammonium nitrate. *J Chem Eng Data* 2012;57:603–9.
33 <https://doi.org/10.1021/je201177t>.
- 34 [230] Cai J, Tao YQ, von Solms N, Xu CG, Chen ZY, Li X Sen. Experimental studies on hydrogen hydrate
35 with tetrahydrofuran by differential scanning calorimeter and in-situ Raman. *Appl Energy*
36 2019;243:1–9. <https://doi.org/10.1016/j.apenergy.2019.03.179>.
- 37 [231] Liu J, Hou J, Xu J, Liu H, Chen G, Zhang J. Ab initio study of the molecular hydrogen occupancy in

- 1 pure H₂ and binary H₂-THF clathrate hydrates. *Int J Hydrogen Energy* 2017;42:17136–43.
2 <https://doi.org/10.1016/j.ijhydene.2017.06.025>.
- 3 [232] Ghaani MR, Takeya S, English NJ. Hydrogen storage in propane-hydrate: Theoretical and
4 experimental study. *Appl Sci* 2020;10:1–10. <https://doi.org/10.3390/app10248962>.
- 5 [233] Zhang Y, Bhattacharjee G, Zheng J, Linga P. Hydrogen storage as clathrate hydrates in the
6 presence of 1,3-dioxolane as a dual-function promoter. *Chem Eng J* 2022;427:131771.
7 <https://doi.org/10.1016/j.cej.2021.131771>.
- 8 [234] Prasad PSR, Sugahara T, Sum AK, Sloan ED, Koh CA. Hydrogen storage in double clathrates with
9 tert-butylamine. *J Phys Chem A* 2009;113:6540–3. <https://doi.org/10.1021/jp9029997>.
- 10 [235] Amano S, Tsuda T, Hashimoto S, Sugahara T, Ohgaki K. Competitive cage occupancy of hydrogen
11 and argon in structure-II hydrates. *Fluid Phase Equilib* 2010;298:113–6.
12 <https://doi.org/10.1016/j.fluid.2010.07.017>.
- 13 [236] Lu H, Wang J, Liu C, Ratcliffe CI, Becker U, Kumar R, et al. Multiple H₂ occupancy of cages of
14 clathrate hydrate under mild conditions. *J Am Chem Soc* 2012;134:9160–2.
15 <https://doi.org/10.1021/ja303222u>.
- 16 [237] Lee S, Lee Y, Park S, Kim Y, Lee JD, Seo Y. Thermodynamic and spectroscopic identification of
17 guest gas enclathration in the double tetra-n-butylammonium fluoride semiclathrates. *J Phys
18 Chem B* 2012;116:9075–81. <https://doi.org/10.1021/jp302647c>.
- 19 [238] Matsumoto M, Tanaka H. On the structure selectivity of clathrate hydrates. *J Phys Chem B*
20 2011;115:8257–65. <https://doi.org/10.1021/jp203478z>.
- 21 [239] Lee BR, Sa JH, Hong SY, Lee JD, Lee KH, Seo Y, et al. Guest-Guest Interactions and Co-Occupation
22 by Distinct Guests in the Metastable State of Clathrate Hydrates. *J Phys Chem C* 2019;123:3811–
23 6. <https://doi.org/10.1021/acs.jpcc.8b08629>.
- 24 [240] Del Rosso L, Celli M, Ulivi L. Raman Measurements of Pure Hydrogen Clathrate Formation from a
25 Supercooled Hydrogen-Water Solution. *J Phys Chem Lett* 2015;6:4309–13.
26 <https://doi.org/10.1021/acs.jpcclett.5b01923>.
- 27 [241] Veluswamy HP, Yew JC, Linga P. New hydrate phase equilibrium data for two binary gas mixtures
28 of hydrogen and propane coupled with a kinetic study. *J Chem Eng Data* 2015;60:228–37.
29 <https://doi.org/10.1021/je500489d>.
- 30 [242] Veluswamy HP, Linga P. Macroscopic kinetics of hydrate formation of mixed hydrates of
31 hydrogen/tetrahydrofuran for hydrogen storage. *Int J Hydrogen Energy* 2013;38:4587–96.
32 <https://doi.org/10.1016/j.ijhydene.2013.01.123>.
- 33 [243] Veluswamy HP, Chen JY, Linga P. Surfactant effect on the kinetics of mixed hydrogen/propane
34 hydrate formation for hydrogen storage as clathrates. *Chem Eng Sci* 2015;126:488–99.
35 <https://doi.org/10.1016/j.ces.2014.12.052>.
- 36 [244] Di Profio P, Canale V, Germani R, Arca S, Fontana A. Reverse micelles enhance the formation of
37 clathrate hydrates of hydrogen. *J Colloid Interface Sci* 2018;516:224–31.
38 <https://doi.org/10.1016/j.jcis.2018.01.059>.

- 1 [245] Oshima M, Shimada W, Hashimoto S, Tani A, Ohgaki K. Memory effect on semi-clathrate hydrate
2 formation: A case study of tetragonal tetra-n-butyl ammonium bromide hydrate. *Chem Eng Sci*
3 2010;65:5442–6. <https://doi.org/10.1016/j.ces.2010.07.019>.
- 4 [246] Zhao J, Wang C, Yang M, Liu W, Xu K, Liu Y, et al. Existence of a memory effect between hydrates
5 with different structures (I, II, and H). *J Nat Gas Sci Eng* 2015;26:330–5.
6 <https://doi.org/10.1016/j.jngse.2015.06.031>.
- 7 [247] Lan R, Irvine JTS, Tao S. Ammonia and related chemicals as potential indirect hydrogen storage
8 materials. *Int J Hydrogen Energy* 2012;37:1482–94.
9 <https://doi.org/10.1016/j.ijhydene.2011.10.004>.
- 10 [248] McKinlay CJ, Turnock SR, Hudson DA. Route to zero emission shipping: Hydrogen, ammonia or
11 methanol? *Int J Hydrogen Energy* 2021;46:28282–97.
12 <https://doi.org/10.1016/j.ijhydene.2021.06.066>.
- 13 [249] Aziz M, TriWijayanta A, Nandiyanto ABD. Ammonia as effective hydrogen storage: A review on
14 production, storage and utilization. *Energies* 2020;13:3062.
15 <https://doi.org/10.3390/en13123062>.

16

17

18